

SM Higgs Boson Measurements with the ATLAS Experiment at 13 TeV

Laurelle Maria Veloce, University of Toronto
On behalf of the ATLAS Collaboration



Higgs Boson Production and Decay at the LHC

Higgs Boson Production at the LHC

- **Gluon-gluon fusion (ggH)**
 - largest cross section
- **Vector boson fusion (VBF)**
 - characterized by presence of two forward jets
- **Associated production with vector boson (VH, V = W/Z)**
 - investigate leptonic decays of W/Z
- **Associated production with tt (ttH)**
 - leptonic decays of top

$$\sigma = 48.6 \text{ pb}$$

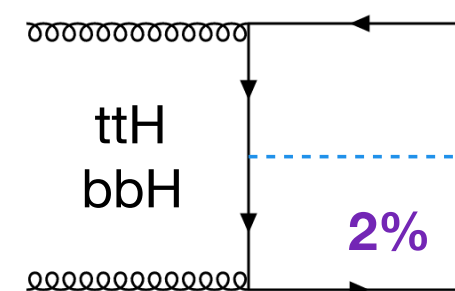
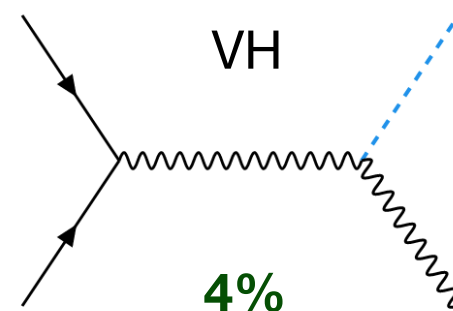
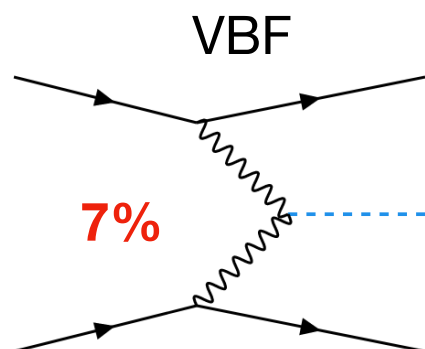
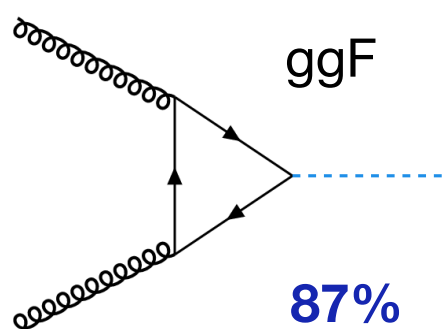
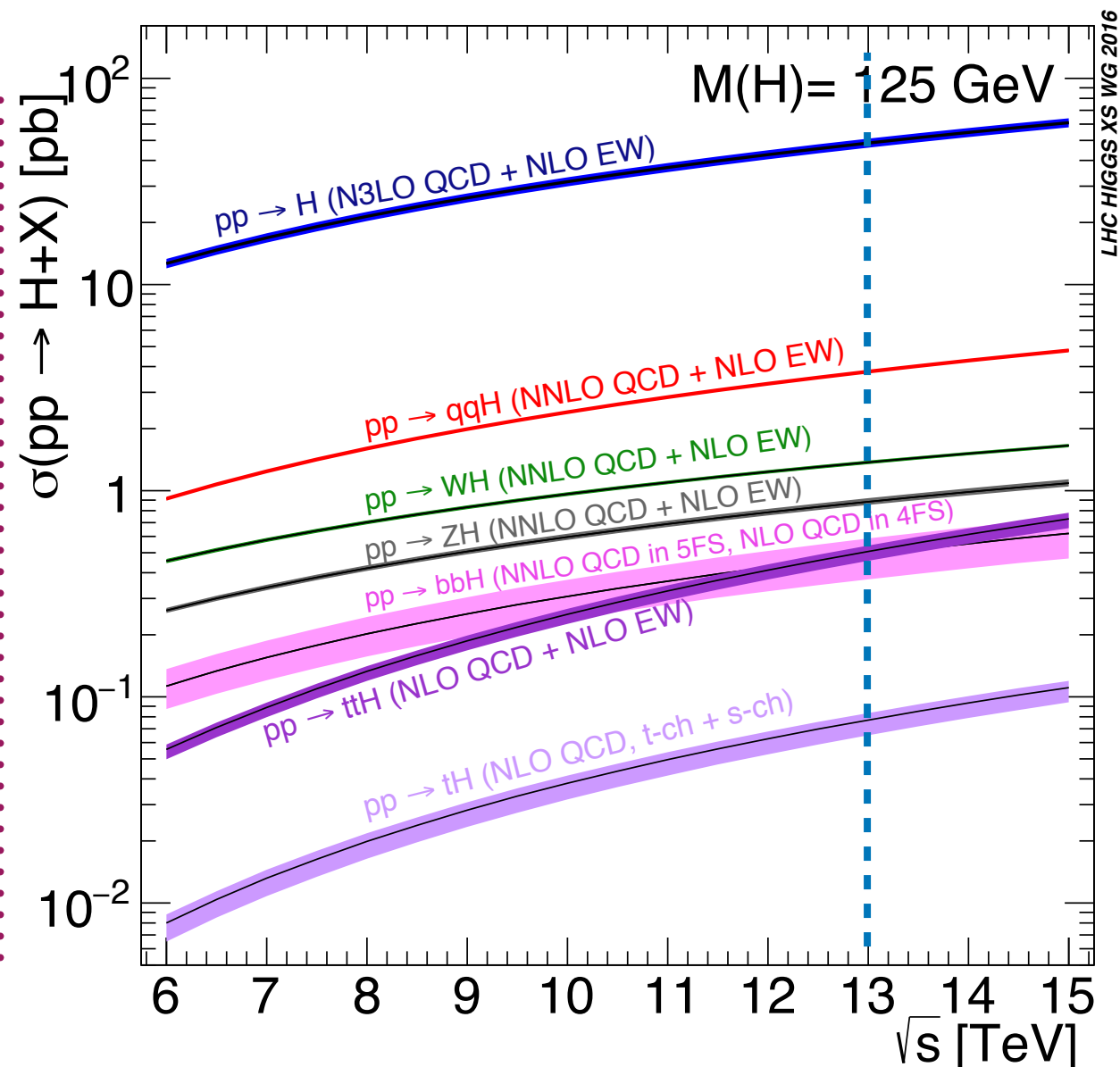
$$\sigma = 3.78 \text{ pb}$$

$$\sigma = 1.37 \text{ pb}$$

$$\sigma = 0.88 \text{ pb}$$

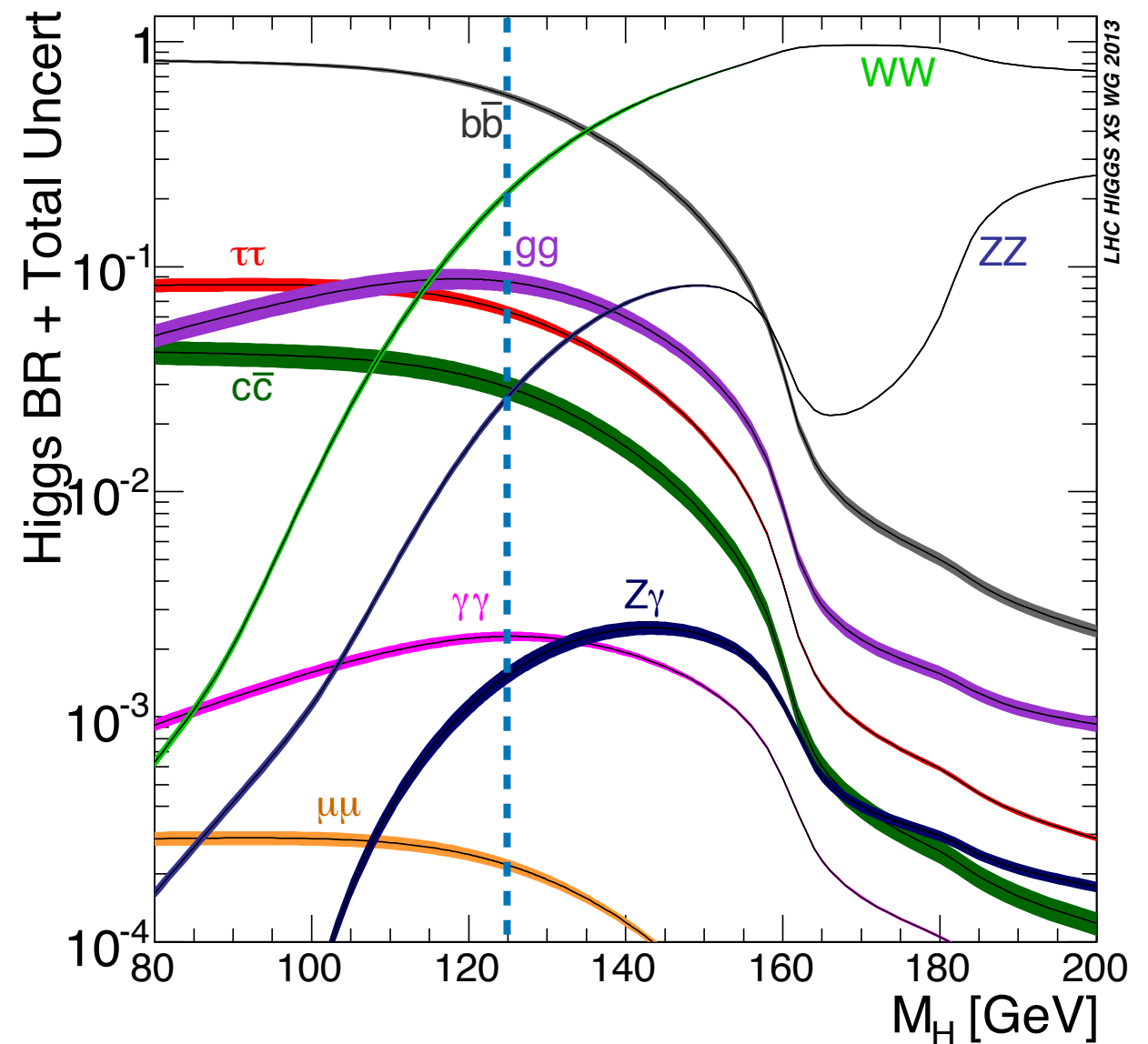
$$\sigma = 0.59 \text{ pb}$$

@ 13 TeV

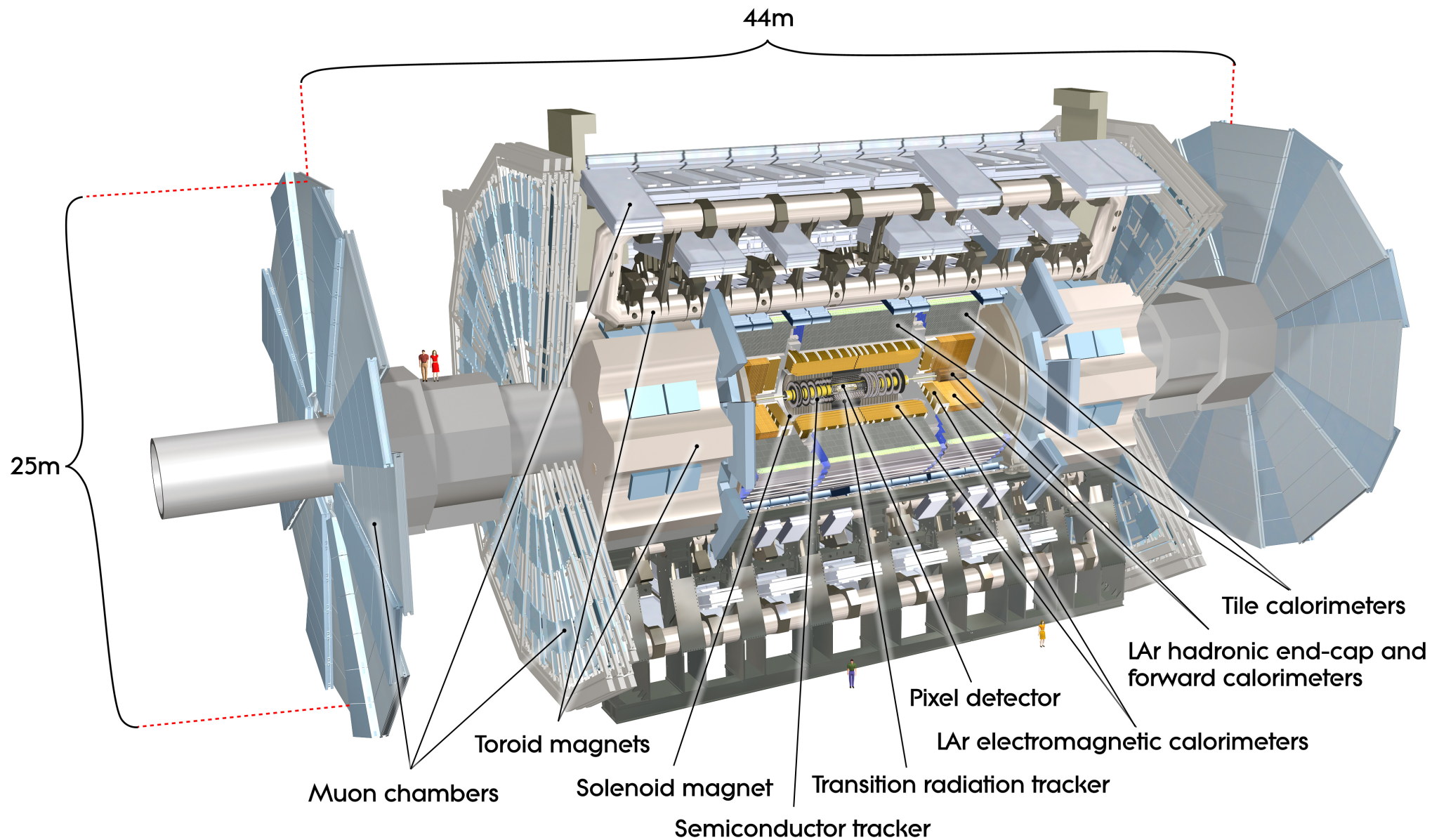


Higgs Boson Decay Modes

- Higgs to boson channels have been observed
 - **ZZ***: low rate, but high signal-to-background ratio
 - **$\gamma\gamma$** : relatively higher rate, but much lower signal-to-background ratio
- **ZZ*** and **$\gamma\gamma$** allow one to fully reconstruct invariant mass of Higgs
- searches for Higgs to fermion decays are challenging
 - **bb**: highest cross section, but very large backgrounds
 - **$\mu\mu$** : very small rate and large background from Drell-Yan



The ATLAS Detector



A general-purpose detector consisting of an inner tracking system, electromagnetic and hadronic calorimeters, and a muon spectrometer

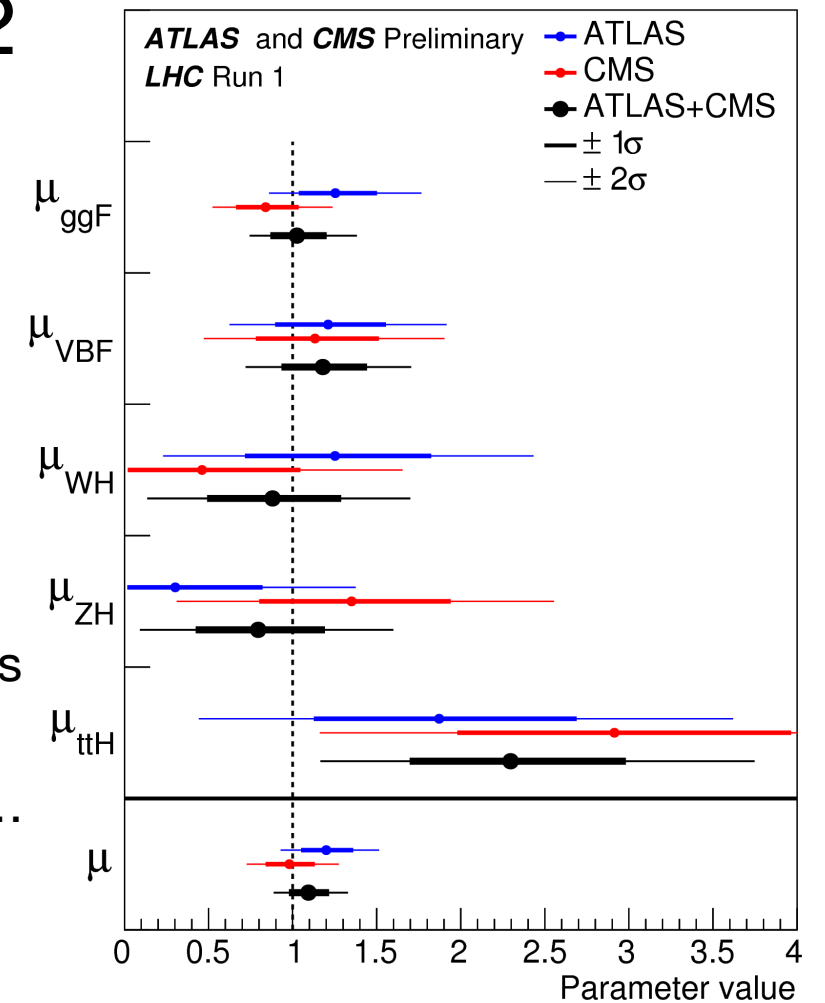
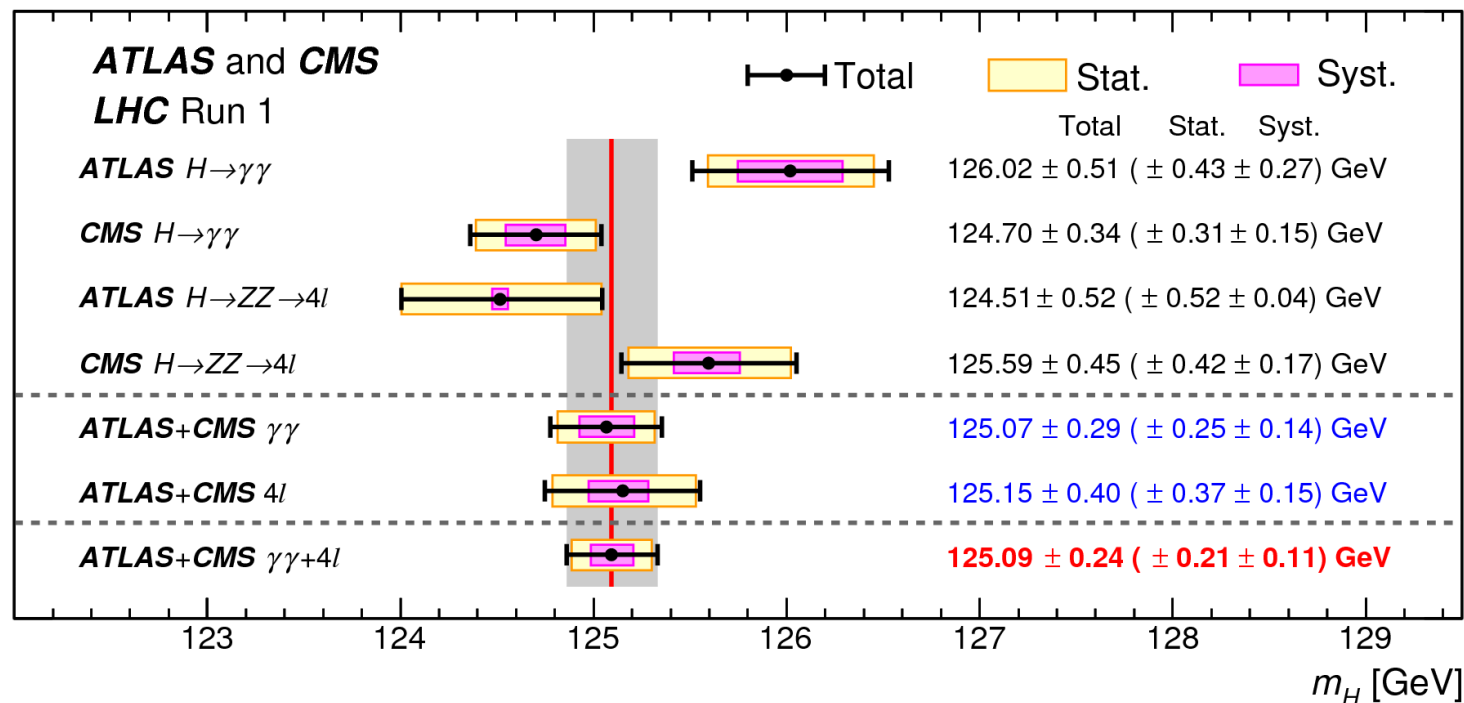
Measurements from $H \rightarrow ZZ^ \rightarrow 4l$
and $H \rightarrow \gamma\gamma$ channels*

125 GeV Higgs candidate announced in 2012

Phys. Lett. B 716 (2012) 1-29

- Results from Run 1 show the new particle to be consistent with a Standard Model Higgs boson
- results shown are for the combined ATLAS and CMS Run 1 results
- but there is still much to do!
 - precision measurements of particle's properties to determine whether it is fully consistent with a SM Higgs
 - production and decay modes still to be observed, including bb , ttH , $\mu\mu$...
 - factor of ~ 2 increase in cross section in Run 2

JHEP 1608 (2016) 045

*Phys. Rev. Lett. 114 (2015) 191803*

Production Modes observed:

- ggH and VBF
- evidence for VH and ttH

Decay modes observed:

- for bosons, $\gamma\gamma$, ZZ, and WW
- for leptons, $\tau\tau$

Once m_H is determined, all other properties of Higgs are fixed

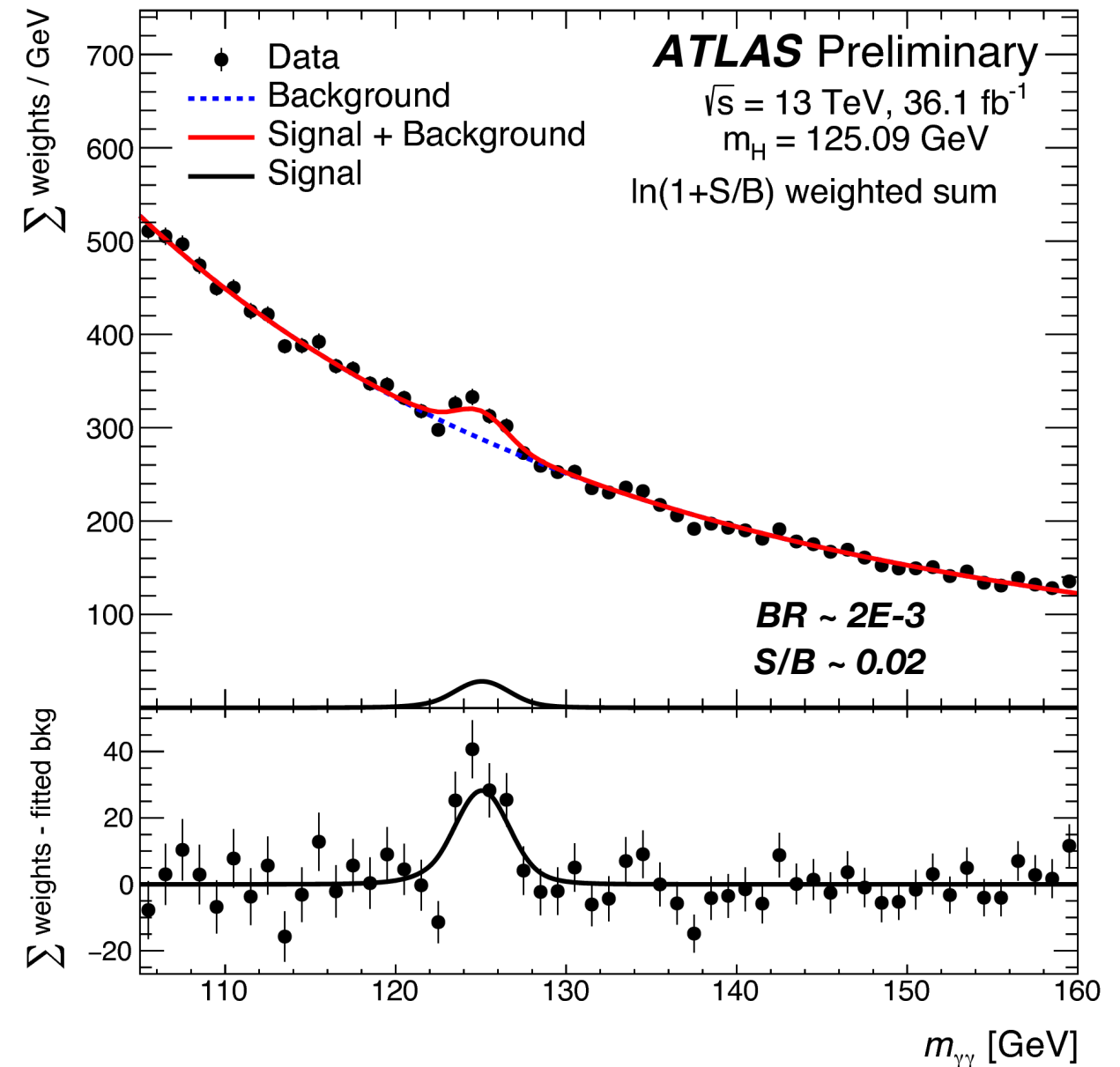
Higgs Boson Measurements

$H \rightarrow \gamma\gamma$

Rare decay ($\sim 0.2\%$), but high resolution results in narrow resonance on top of smoothly falling background

Selection Cuts:

- At least two photon candidates
- Photons must be isolated, fall within $|\eta| < 2.37$, and with $E_{\text{TM}\gamma\gamma} > 0.35$ and $E_{\text{TM}\gamma\gamma} > 0.25$
- *Important backgrounds include $\gamma\gamma$ production, γ -jet production, and dijet production*
- an unbinned likelihood fit is performed on $m_{\gamma\gamma}$
- continuum background is obtained from data



$$m_H = 125.11 \pm 0.42 \text{ GeV}$$

Higgs Boson Measurements

$$H \rightarrow ZZ^* \rightarrow |+-|+|-$$

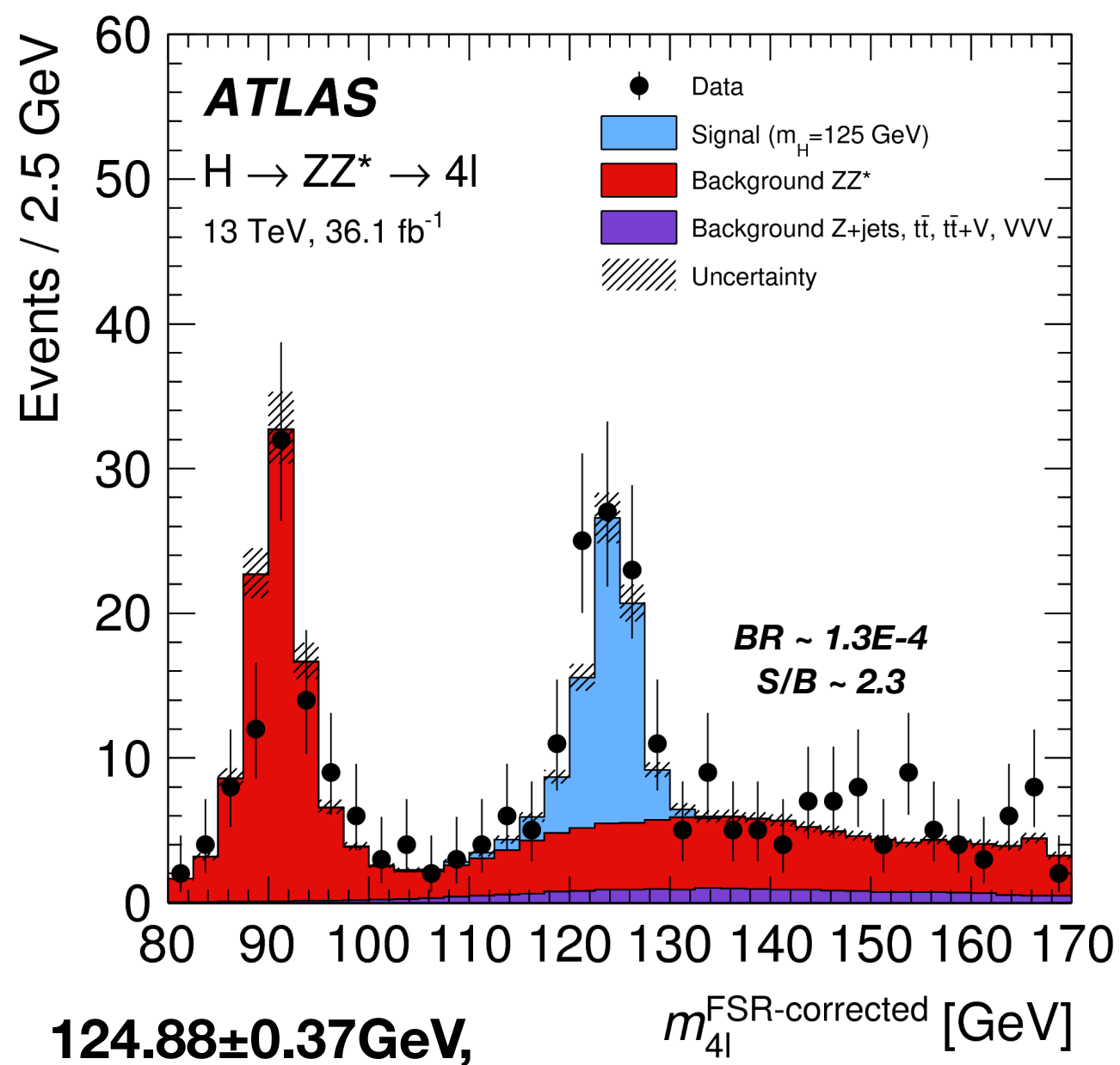
low branching ratio, but high S/B for all four final states (4mu, 4e, 2mu2e, 2e2mu)

Selection Cuts:

- 2 pairs of isolated, same-flavour, oppositely-charged leptons, with one lepton pair close to the Z mass

Important backgrounds include ZZ continuum, as well as contributions from Z+jets and tt-bar*

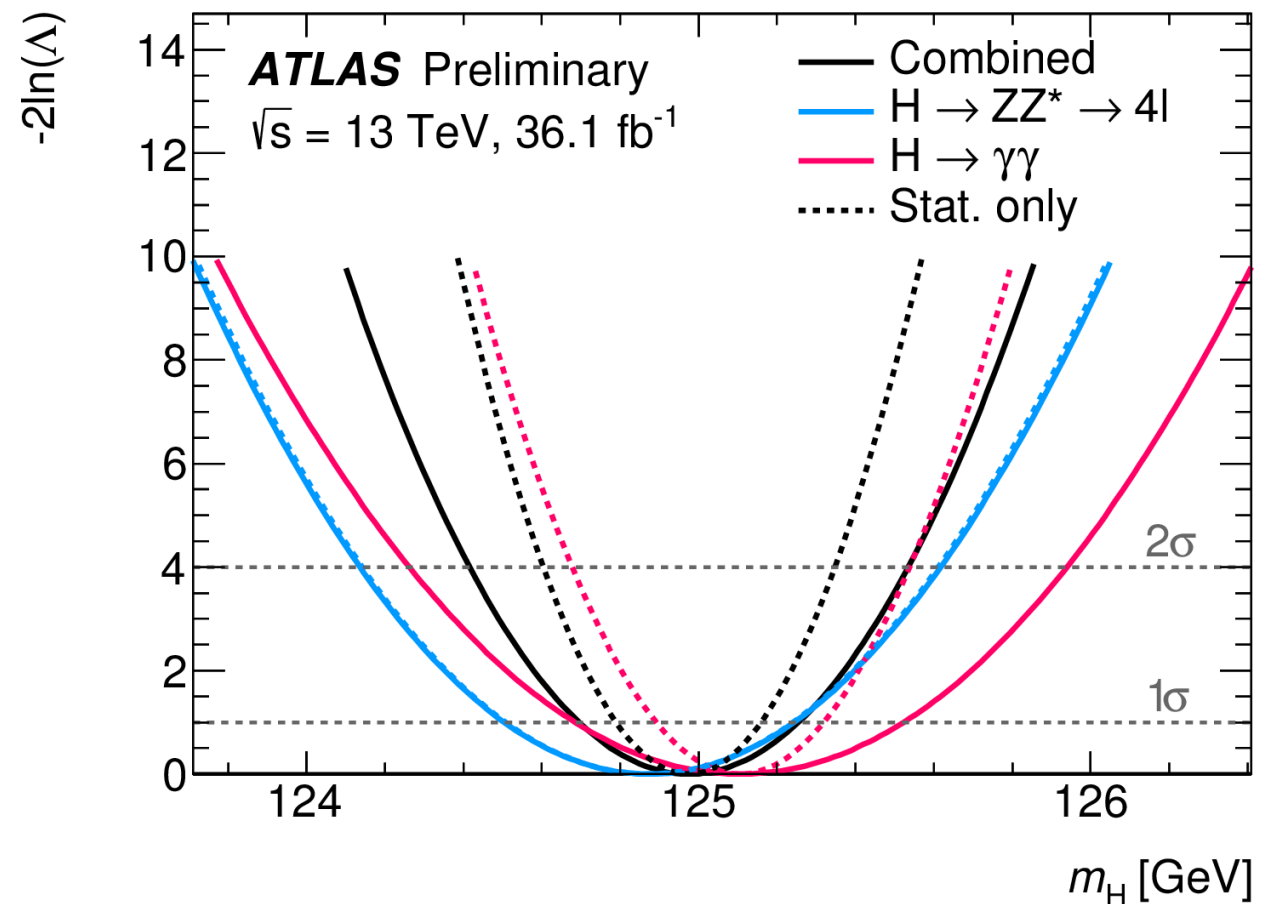
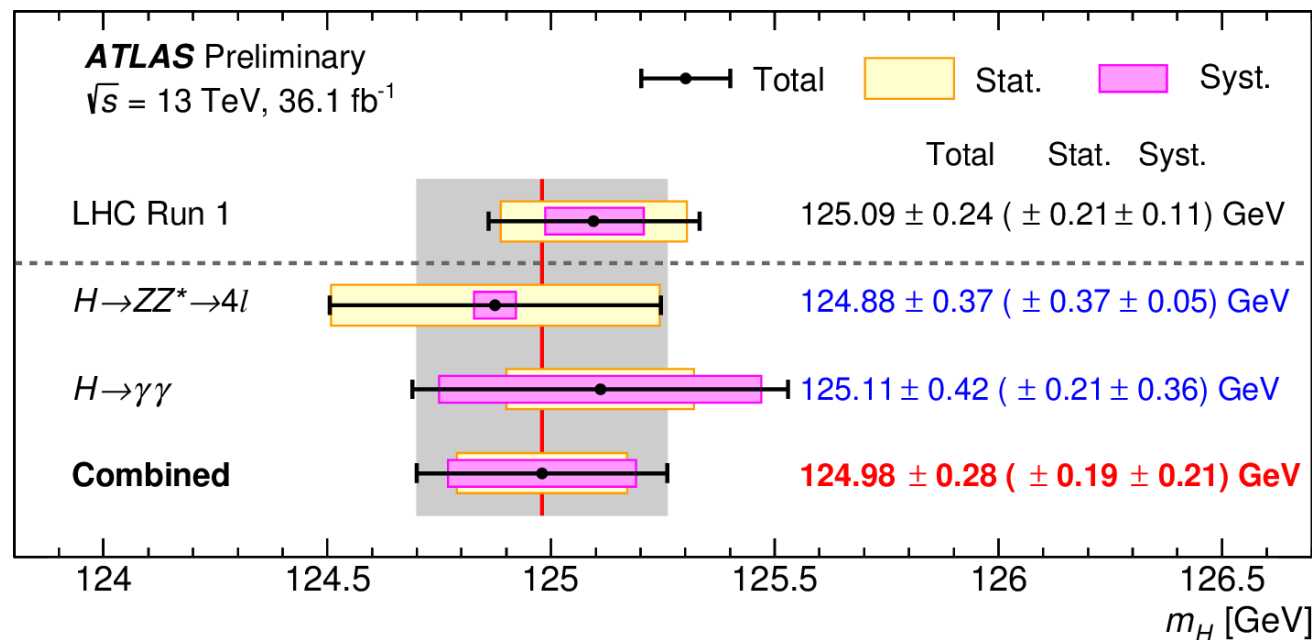
- per-event method for mass determination
- continuum background is obtained from MC, while Z+jets and ttbar from data



$$m_H = 124.8 \pm 0.37 \text{ GeV}$$

Higgs Boson mass measurement in $H \rightarrow ZZ^* \rightarrow 4l$ and $H \rightarrow \gamma\gamma$ channels

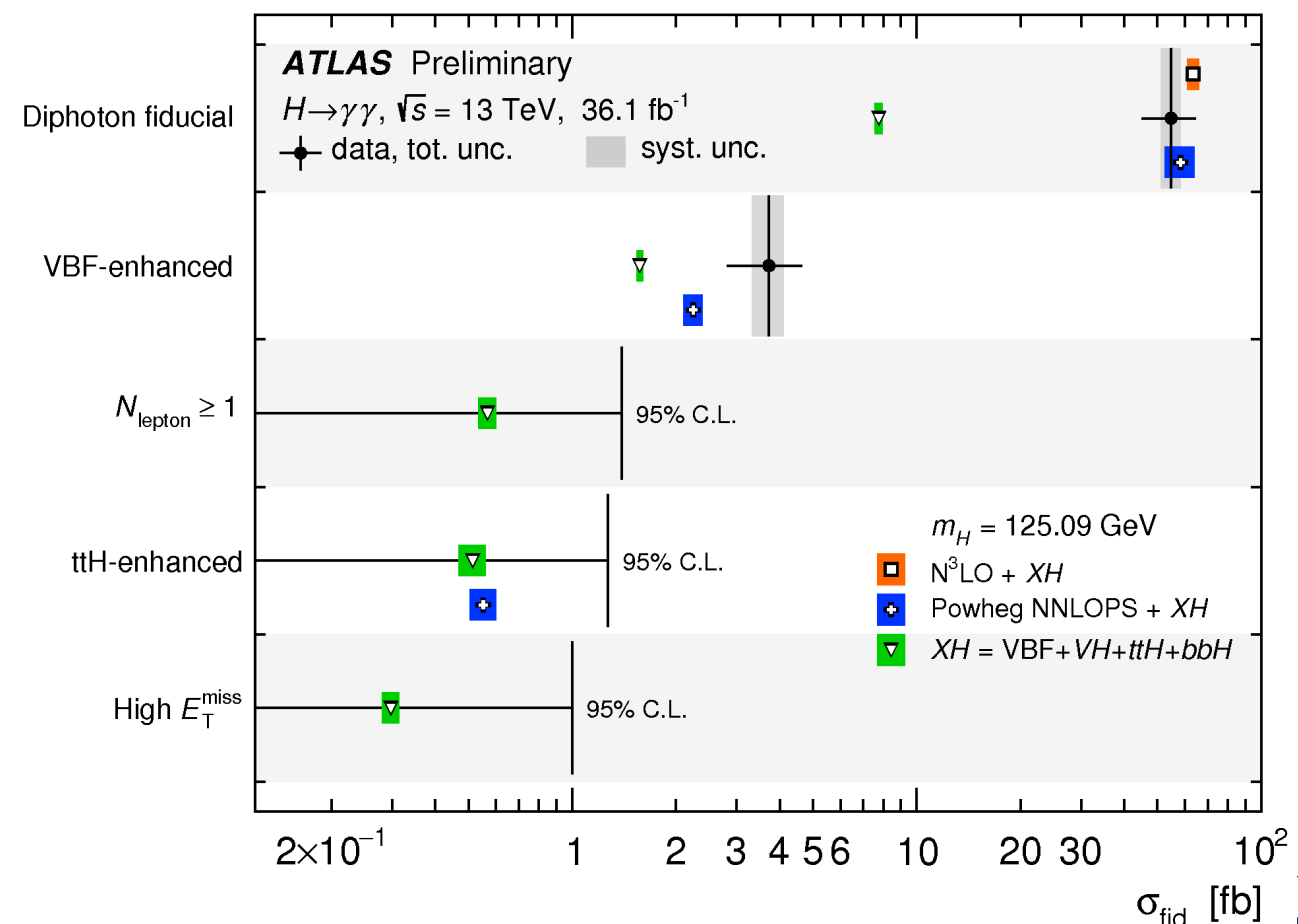
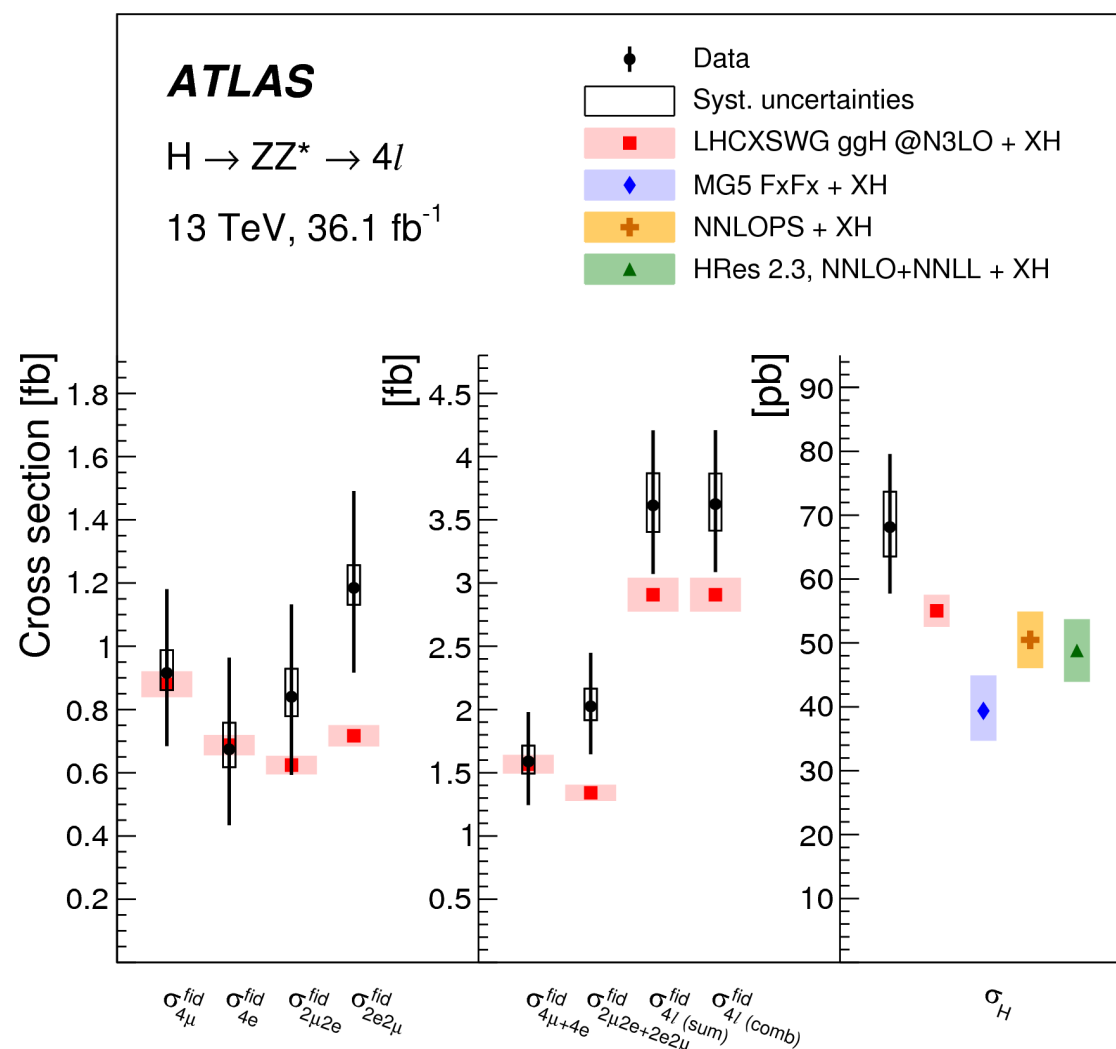
- m_H not predicted in the SM, but once measured, all other properties are fixed
- therefore a precise measurement is required to investigate the Standard Model in detail
- mass measurement is performed in two channels with high mass resolution ($\sim 1-2\%$) due to fully reconstructed final states



$$m_H = 124.98 \pm 0.28 \text{ GeV}$$

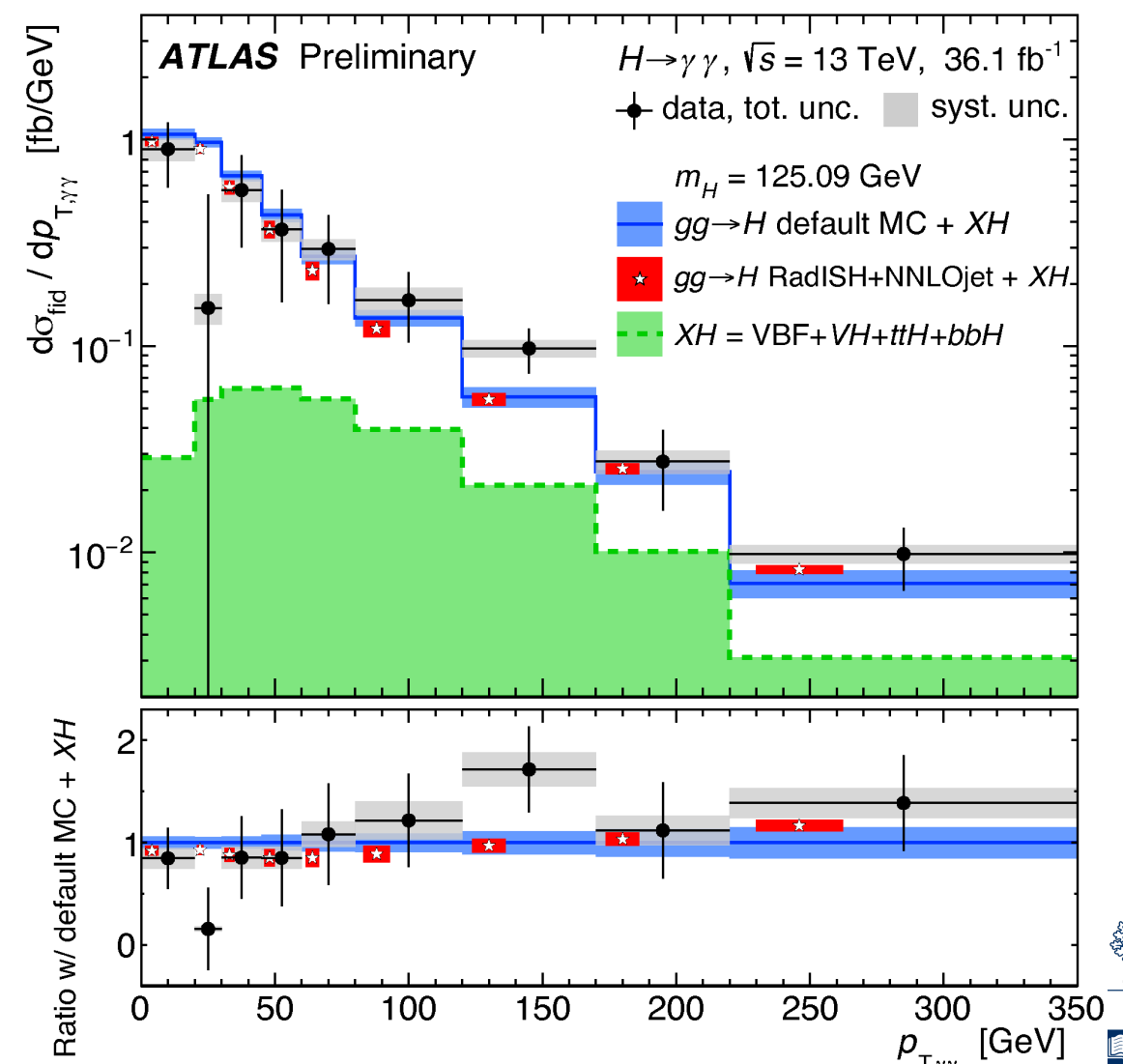
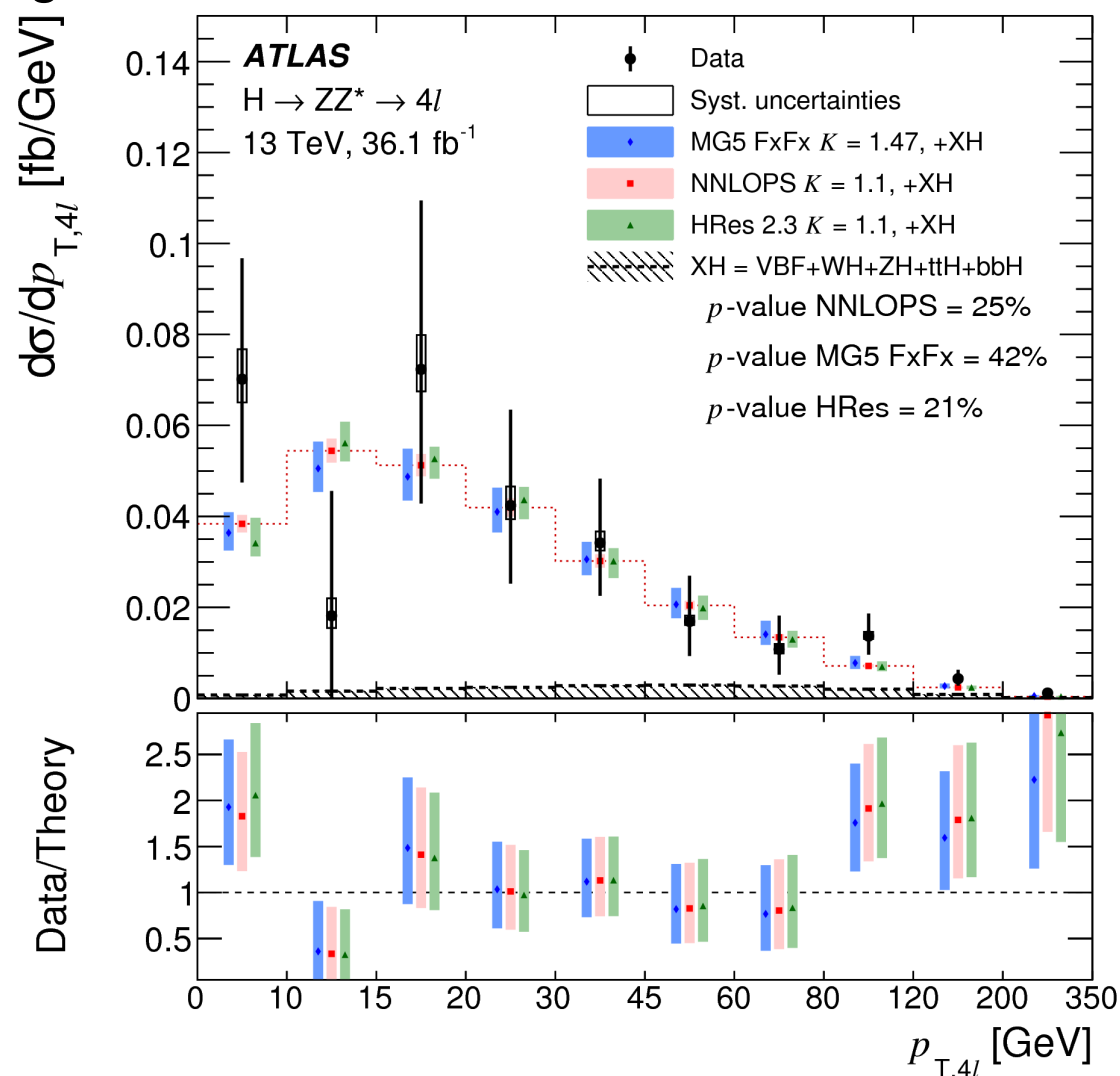
Higgs Boson fiducial and total cross sections in $H \rightarrow ZZ^* \rightarrow 4l$ and $H \rightarrow \gamma\gamma$ channels

- measure cross sections in fiducial region which closely follows the kinematic and selection cuts to reduce model dependency in extrapolation
- reconstruction acceptance relative to fiducial is high (50% ($H4l$), 75% ($H\gamma\gamma$))
- correct for detector effects by “unfolding”; performed bin-by-bin
- agreement with SM



Higgs Boson fiducial and total cross sections in $H \rightarrow ZZ^* \rightarrow 4l$ and $H \rightarrow \gamma\gamma$ channels

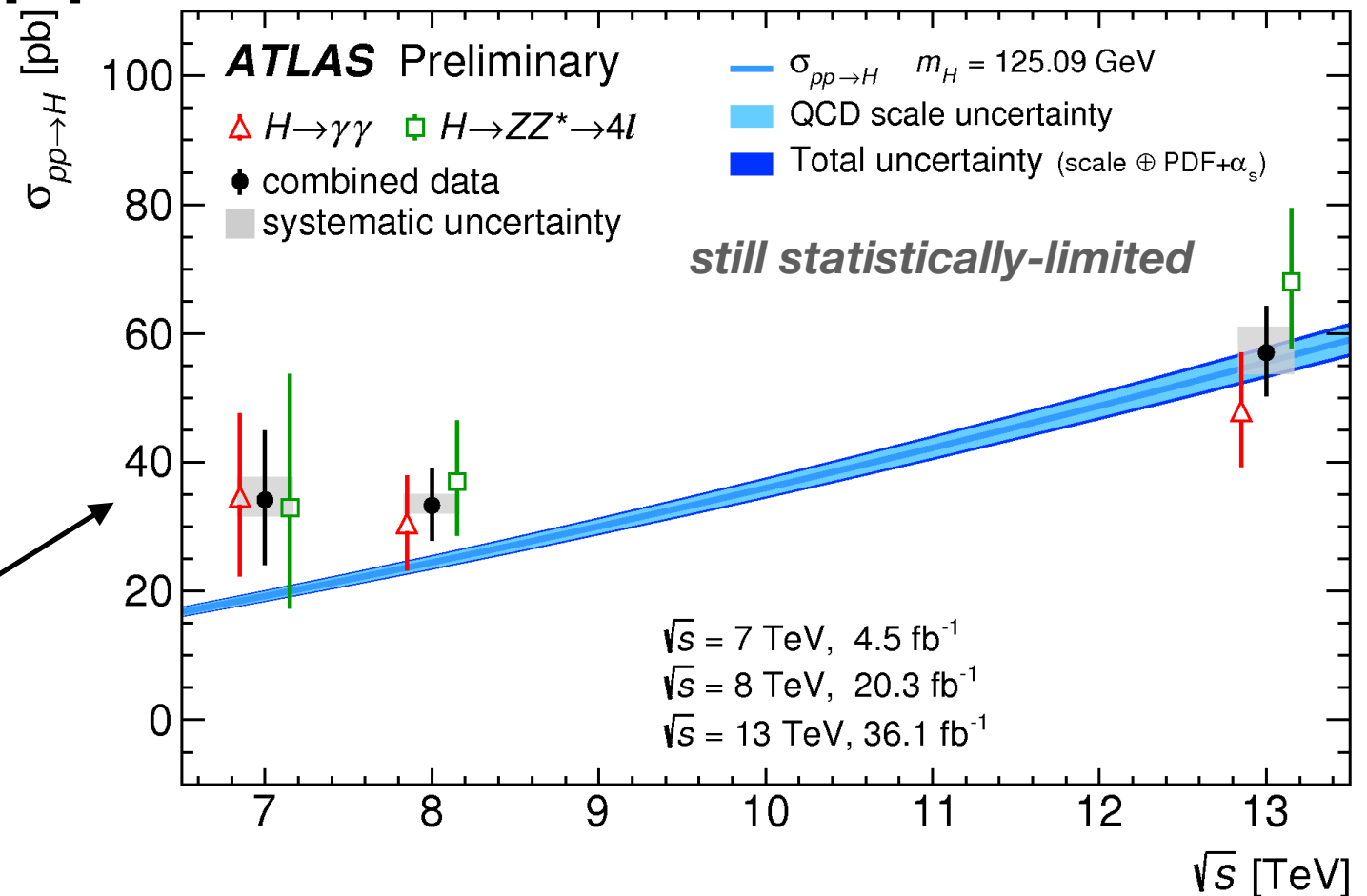
- measure cross sections in fiducial region which closely follows the kinematic and selection cuts to reduce model dependency in extrapolation
- reconstruction acceptance relative to fiducial is high (50% ($H4l$), 75% ($H\gamma\gamma$))
- correct for detector effects by “unfolding”; performed bin-by-bin
- agreement with SM



Higgs Boson fiducial and total cross sections in $H \rightarrow ZZ^* \rightarrow 4l$ and $H \rightarrow \gamma\gamma$ channels

- total cross section is based on inclusive event yields
- assumes Standard Model cross-section ratios and branching ratios

combined total cross section compared to N3LO QCD prediction for $m_H = 125.09$ GeV

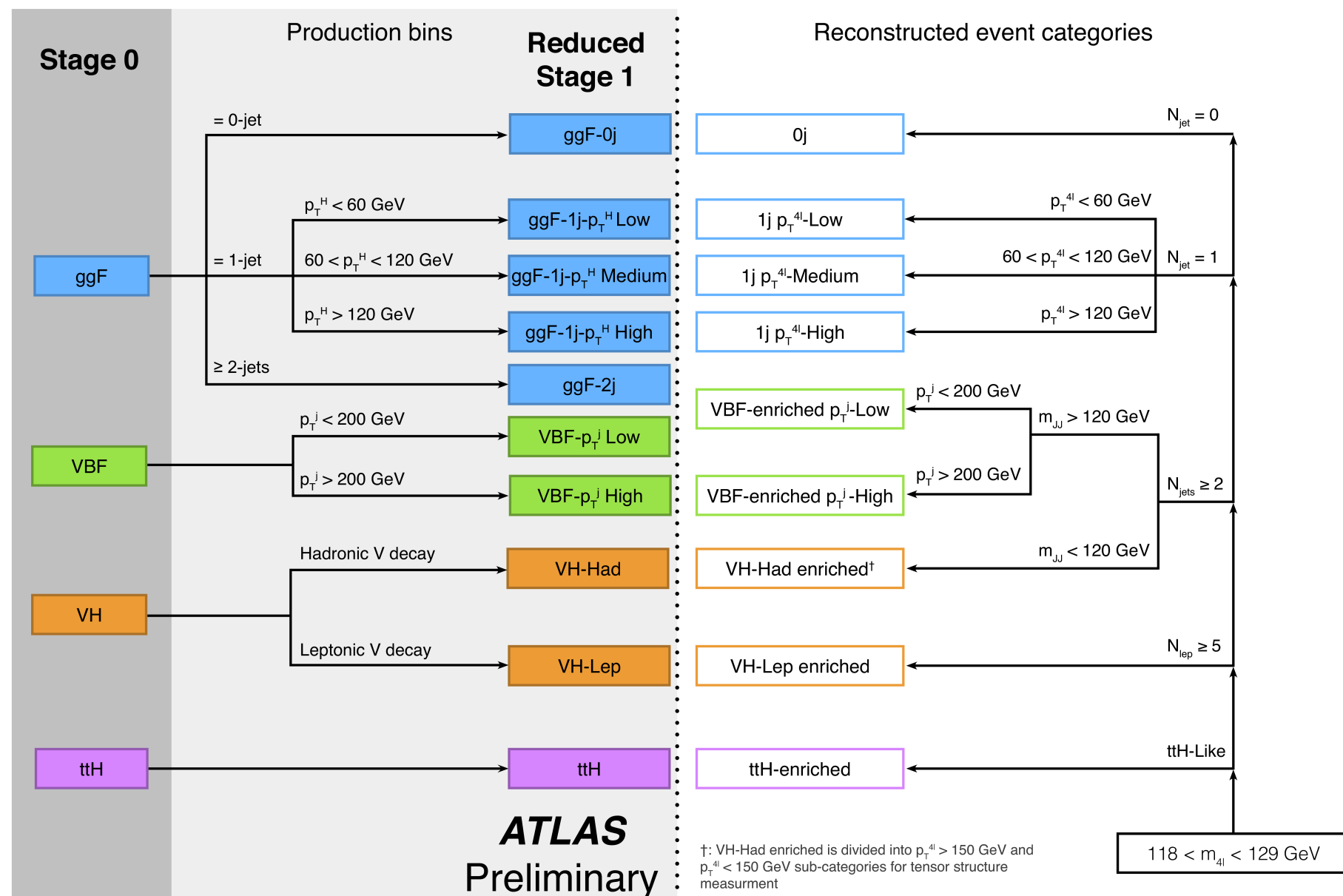


Decay channel	Total cross section ($pp \rightarrow H + X$)		
	$\sqrt{s} = 7$ TeV	$\sqrt{s} = 8$ TeV	$\sqrt{s} = 13$ TeV
$H \rightarrow \gamma\gamma$	35^{+13}_{-12} pb	$30.5^{+7.5}_{-7.4}$ pb	$47.9^{+9.1}_{-8.6}$ pb
$H \rightarrow ZZ^* \rightarrow 4l$	33^{+21}_{-16} pb	37^{+9}_{-8} pb	$68.0^{+11.4}_{-10.4}$ pb
Combination	34 ± 10 (stat.) $^{+4}_{-2}$ (syst.) pb	$33.3^{+5.5}_{-5.3}$ (stat.) $^{+1.7}_{-1.3}$ (syst.) pb	$57.0^{+6.0}_{-5.9}$ (stat.) $^{+4.0}_{-3.3}$ (syst.) pb
SM prediction [8]	19.2 ± 0.9 pb	24.5 ± 1.1 pb	$55.6^{+2.4}_{-3.4}$ pb

Higgs boson Simplified Template Cross Sections measurements for $H \rightarrow ZZ^* \rightarrow 4l$ and $H \rightarrow \gamma\gamma$

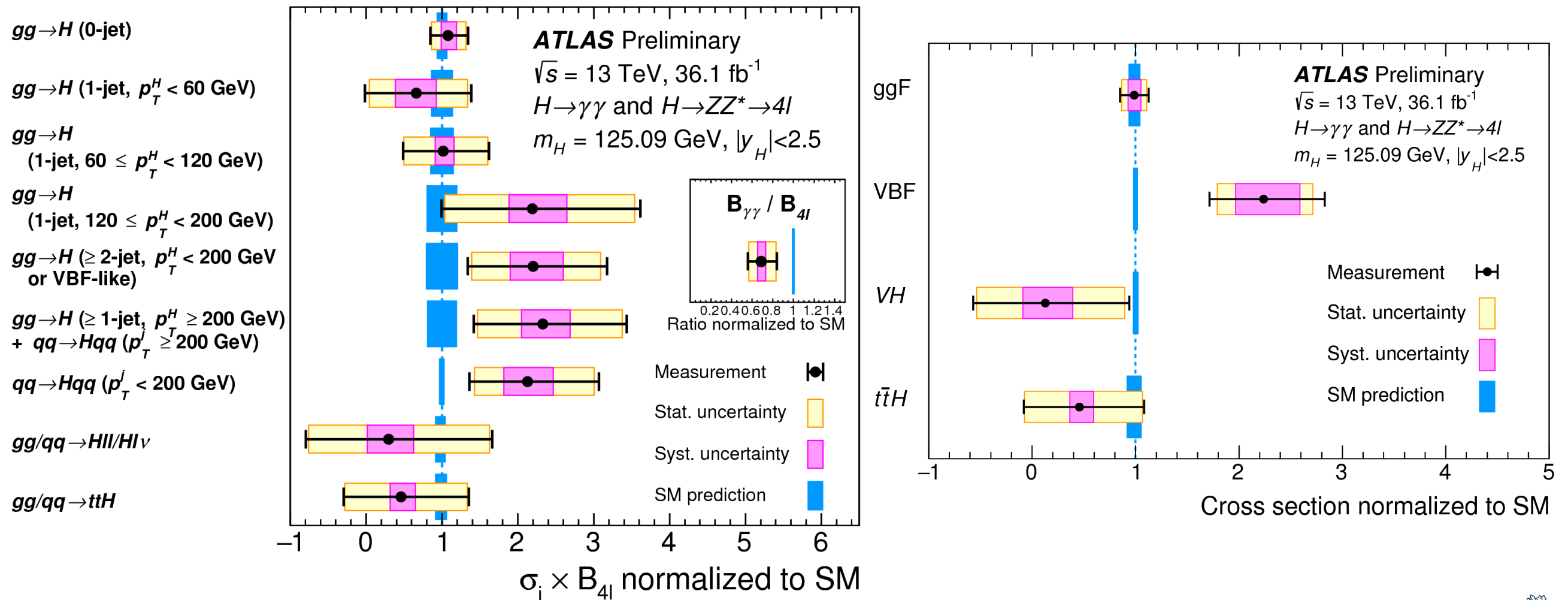
- measure different production cross sections (xBR) in exclusive regions of phase space
 - maximize measurement precision and sensitivity to new physics
 - avoid model-dependent extrapolation

Example from $H4l$



Higgs boson Simplified Template Cross Sections measurements for $H \rightarrow ZZ^* \rightarrow 4l$ and $H \rightarrow \gamma\gamma$

- fit results normalized to SM predictions



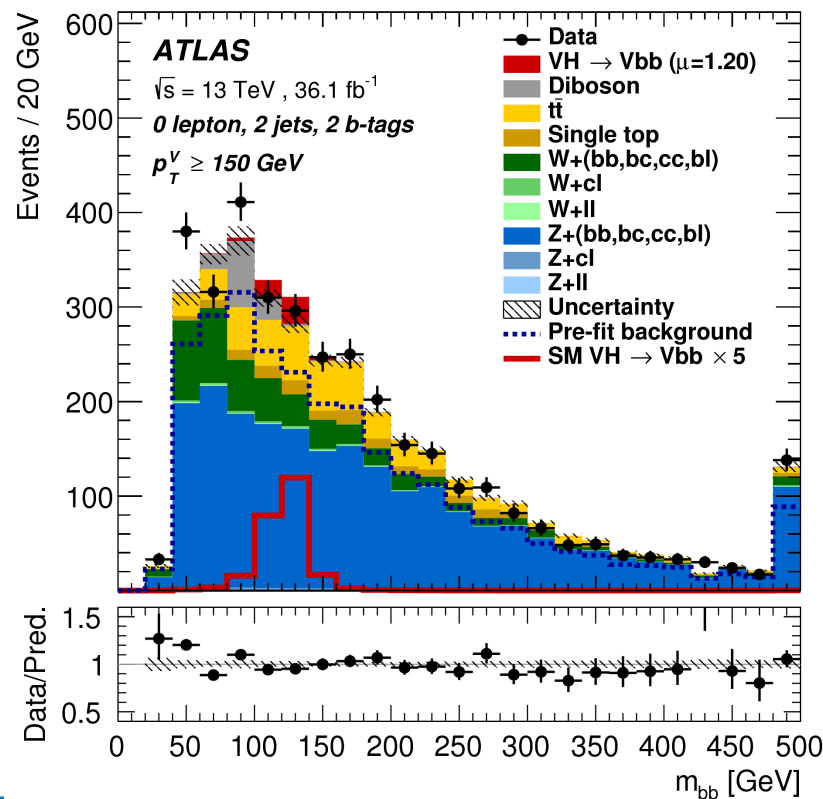
Global Signal Strength: $\mu_H = 1.09 \pm 0.12$

New Results for Higgs to Fermion Decays

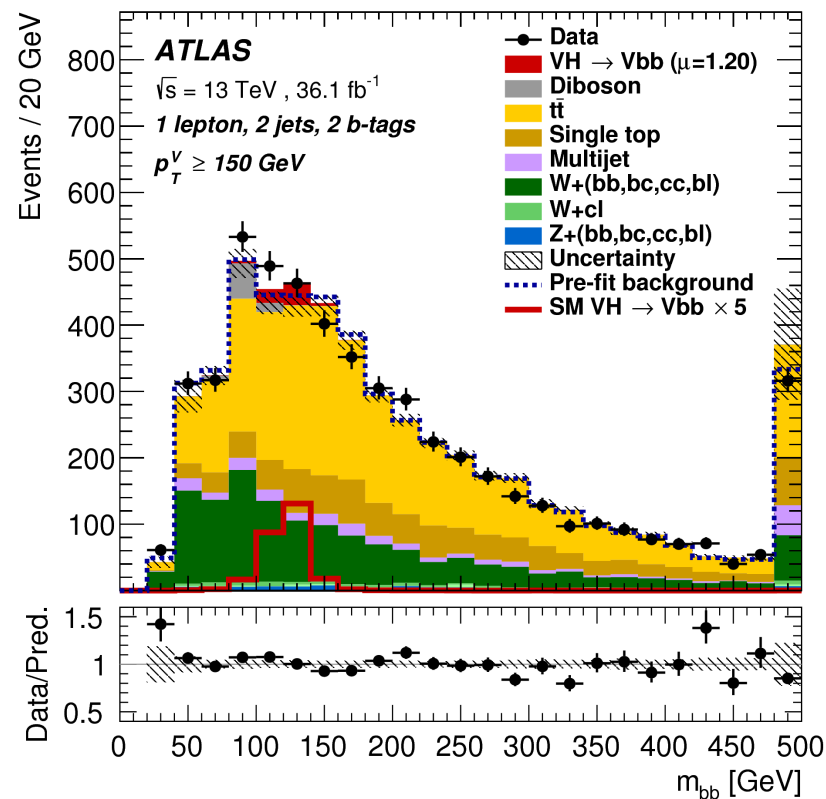
Evidence for $H \rightarrow bb$ decay

- $H \rightarrow bb$ is the most common decay of the Higgs (58% for $m_H = 125$ GeV)
- very large backgrounds from multi-jet production
 - tag events via Higgs produced in association with leptonic W or Z

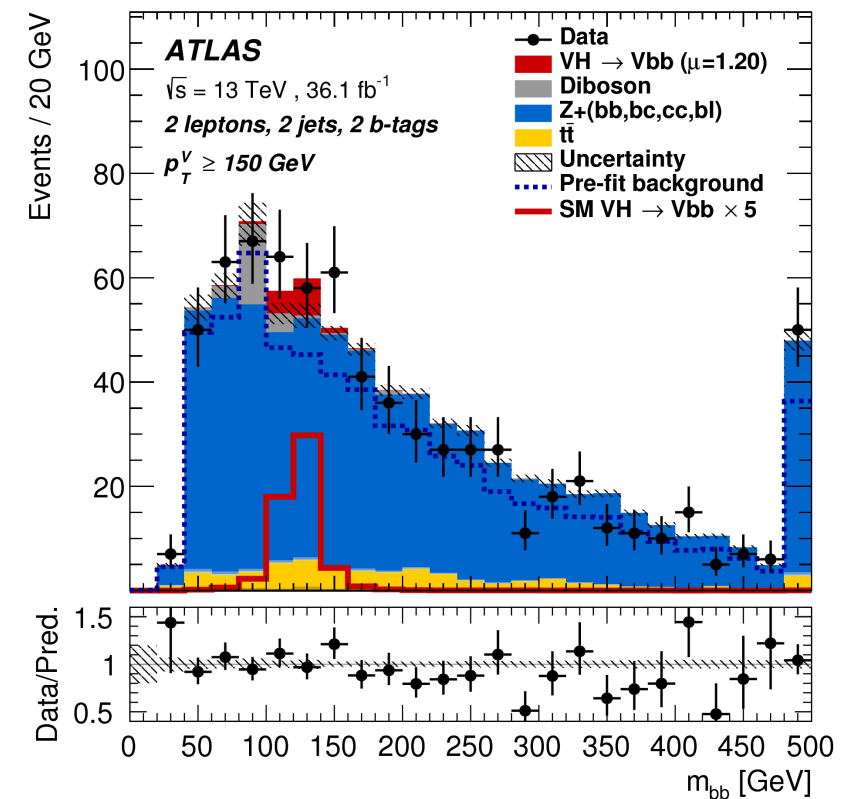
ZH \rightarrow $\nu\nu bb$



WH \rightarrow $l\nu bb$

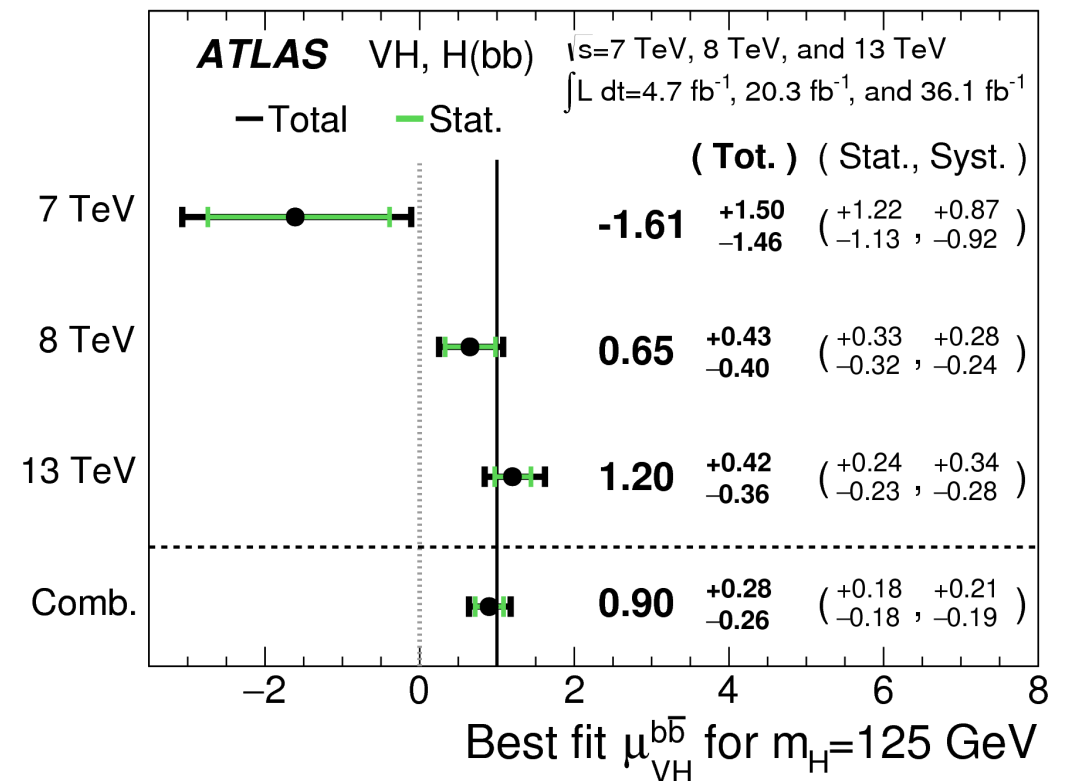
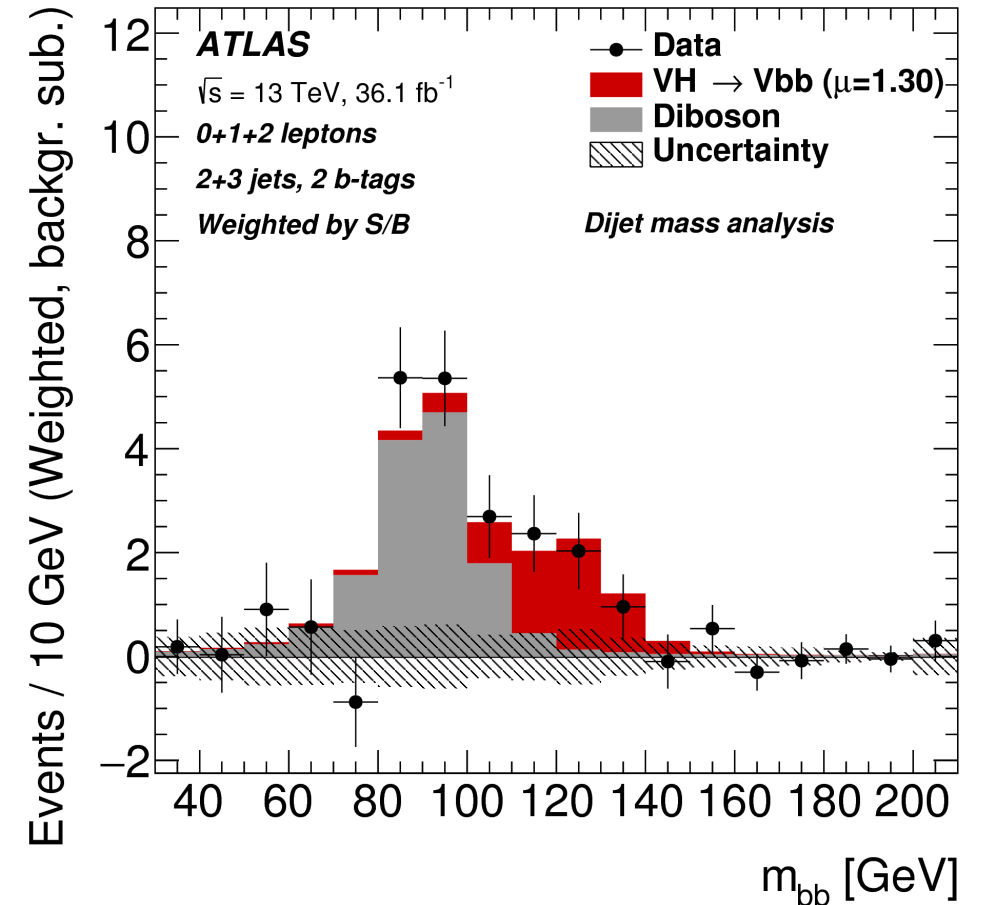
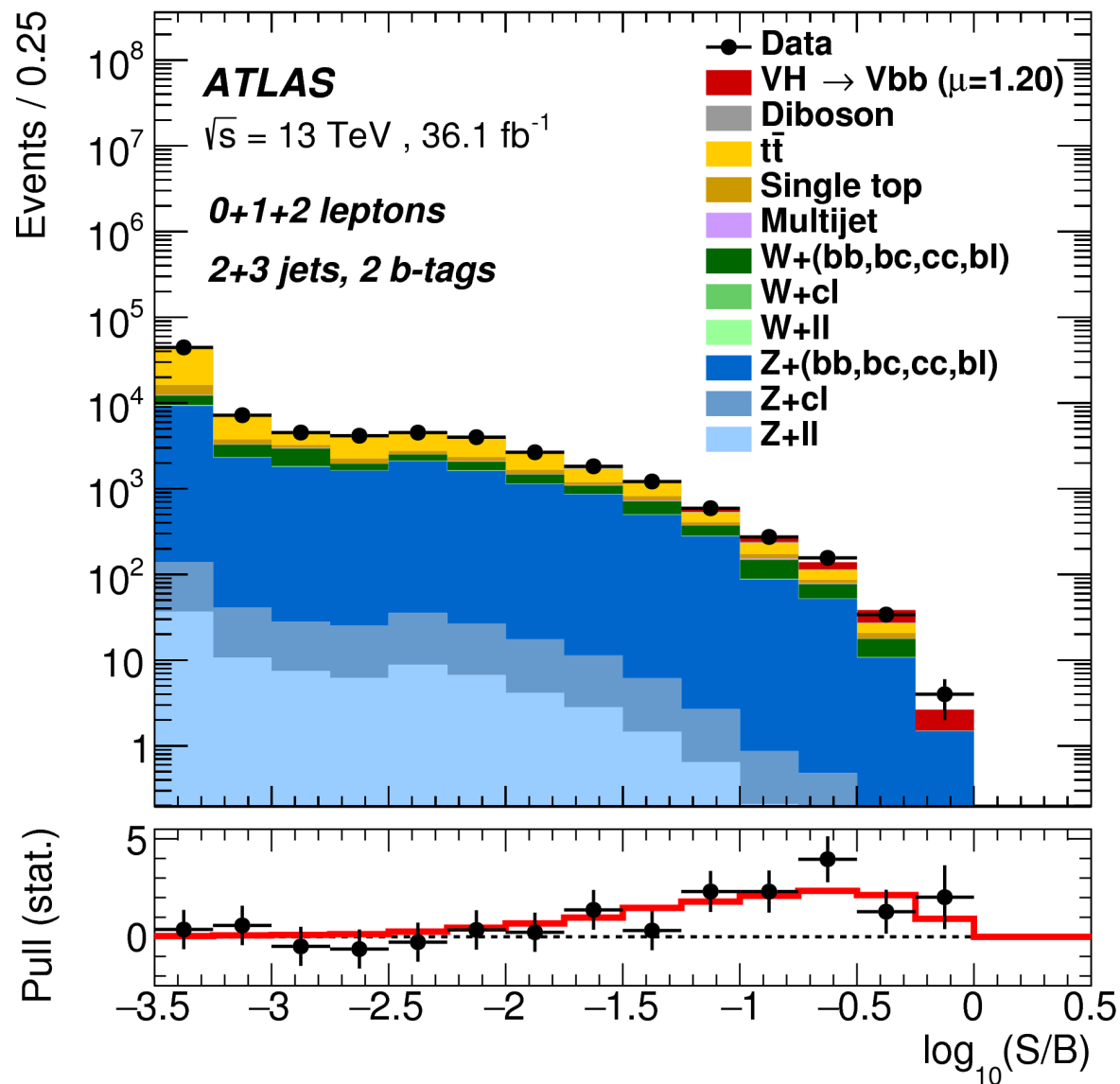


ZH \rightarrow $ll bb$



Evidence for $H \rightarrow bb$ decay

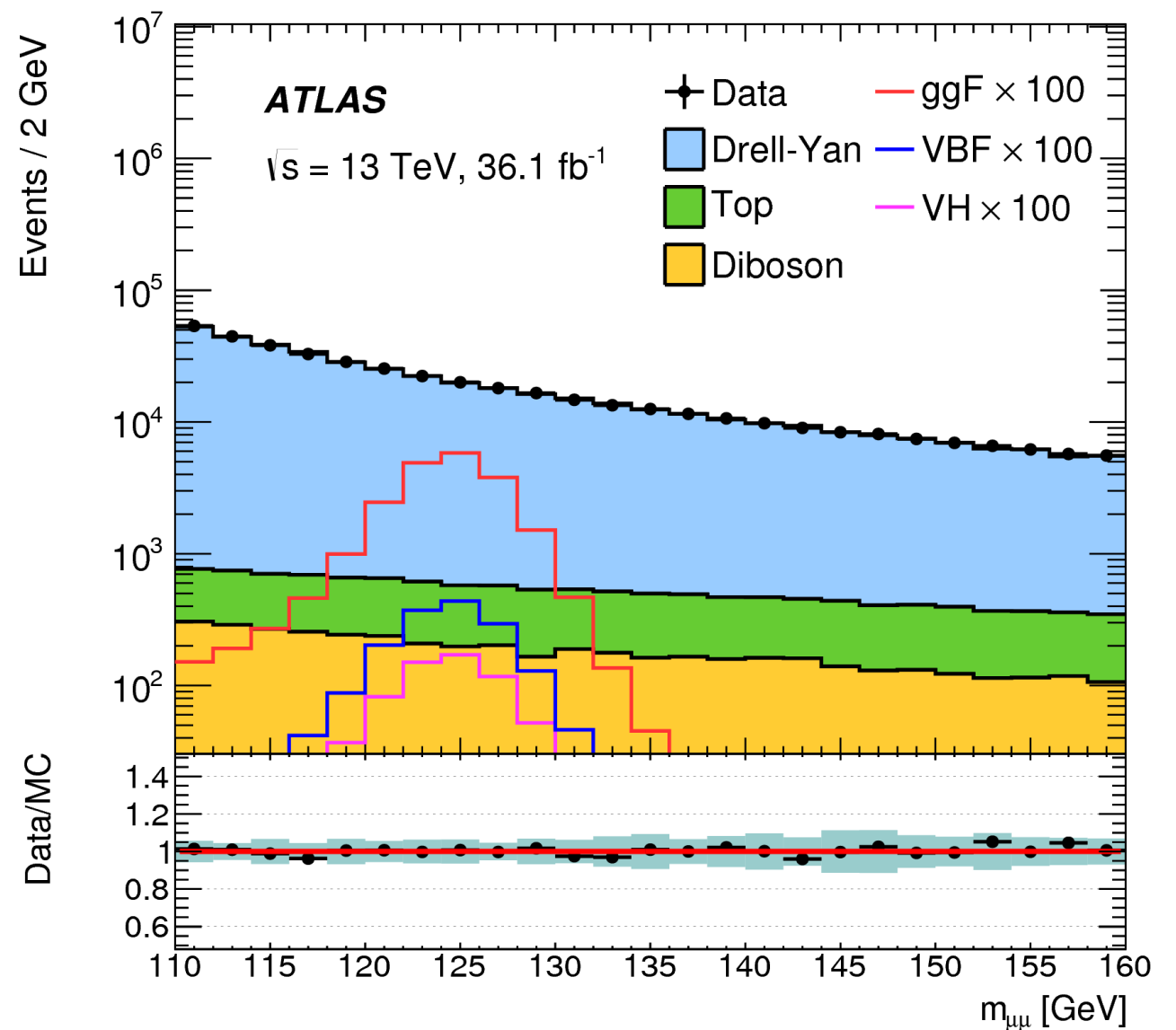
- event kinematics and topology are combined into a multivariate discriminant
- binned maximum-likelihood fit applied to all categories and channels simultaneously
- additional dijet-mass analysis and validation via diboson analysis
 - see clear excess of VZ , $Z \rightarrow bb$ events in the diboson analysis, with a significance of 5.8σ (5.3σ)



Run 2 significance observed (expected):
 3.5σ (3.0σ); combined with Run 1, 3.6σ (4.0σ)

Search for $H \rightarrow \mu\mu$ decay

- challenging due to the very low S/B (0.022% BR!)
- BDT is used to select for VBF-like events
- events are split into categories according to transverse momentum and pseudo-rapidity of muons
- fit the $m_{\mu\mu}$ distribution over 110-160 GeV range using an analytical S+B model
- no evidence yet for Higgs to muon decays



Observed (expected) limit for 125 GeV Higgs:
 3.0 (3.1) for 95% C.L., combined with Run 1, 2.8
 (2.9), times the SM prediction

Conclusions and Outlook

- comprehensive strategy to investigate the Standard Model nature of the 125 GeV Higgs
- updated results for channels with more statistics
- no significant deviations from Standard Model expectations
- new results on Higgs decays to bb and $\mu\mu$
- More measurements to come - stay tuned!

Reference List

13 TeV Combination

- ATLAS, “Measurement of the Higgs boson mass in the $H \rightarrow ZZ \rightarrow 4l$ and $H \rightarrow \gamma\gamma$ channels with $\sqrt{s} = 13$ TeV pp collisions using the ATLAS detector
- ATLAS, “Combined measurements of Higgs boson production and decay in $H \rightarrow ZZ \rightarrow 4l$ and $H \rightarrow \gamma\gamma$ channels using $\sqrt{s} = 13$ TeV pp collision data collected with the ATLAS experiment”, ATLAS-CONF-2017-047, (2017).

Higgs Boson Discovery

- CERN, “Measurements of the Higgs boson production and decay rates and constraints on its couplings from a combined ATLAS and CMS analysis of the LHC pp collision data at $\sqrt{s} = 7$ and 8 TeV” ATLAS-CONF-2015-044, (2015).
- ATLAS & CMS, “Combined Measurement of the Higgs Boson Mass in pp Collisions at $\sqrt{s} = 7$ and 8 TeV with the ATLAS and CMS Experiments”, Phys. Rev. Lett. 114, 191803, (2015).

$H \rightarrow ZZ \rightarrow 4l$

- ATLAS, “Measurement of the Higgs boson coupling properties in the $H \rightarrow ZZ \rightarrow 4l$ decay channel at $\sqrt{s} = 13$ TeV with the ATLAS detector”, ATLAS-CONF-2017-043 (2017).
- ATLAS, “Measurement of inclusive and differential cross section in the $H \rightarrow ZZ \rightarrow 4l$ decay channel in pp collisions at $\sqrt{s} = 13$ TeV with the ATLAS detector”, arXiv:1708.02810, (2017).

$H \rightarrow \gamma\gamma$

- ATLAS, “Measurement of Higgs boson properties in the diphoton decay channel with 36.1 fb⁻¹ collision data at the center-of-mass energy of 13 TeV with the ATLAS detector”, ATLAS-CONF-2017-045, (2017).

Fermion Decays

- ATLAS, “Search for the dimuon decay of the Higgs boson in pp collisions at $\sqrt{s} = 13$ TeV with the ATLAS detector”, Phys. Rev. Lett. **119**, 051802 (2017).
- ATLAS, “Evidence for the $H \rightarrow bb$ decay with the ATLAS detector”, arXiv:1708.03299 (2017).

Backup

Particle Signatures in ATLAS

Electrons

Electron Calorimeter

Photons

Electron Calorimeter

Muons

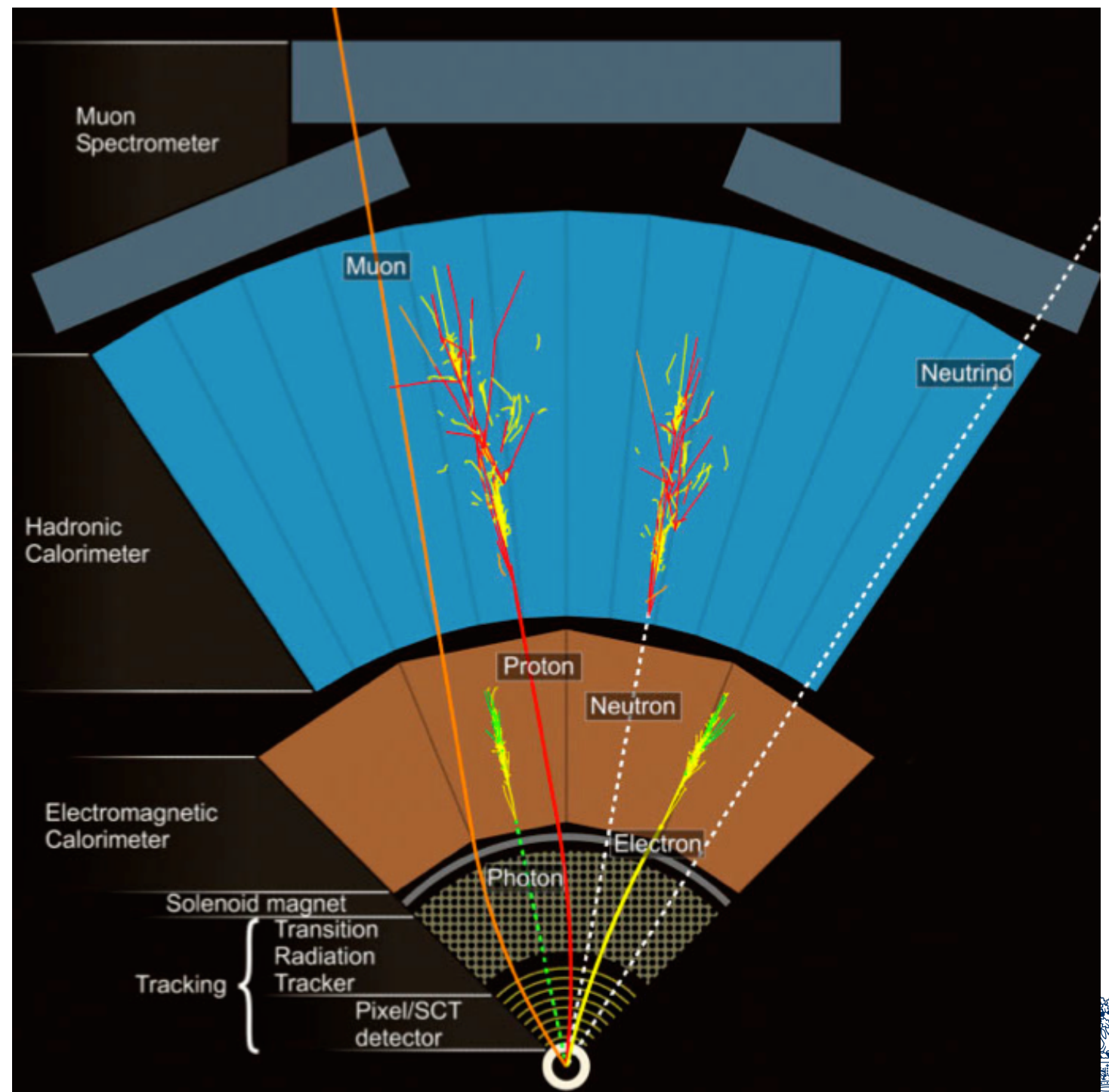
Inner Detector + Muon
Spectrometer

Neutrinos

Missing Energy

Hadrons (Jets)

Hadronic Calorimeter



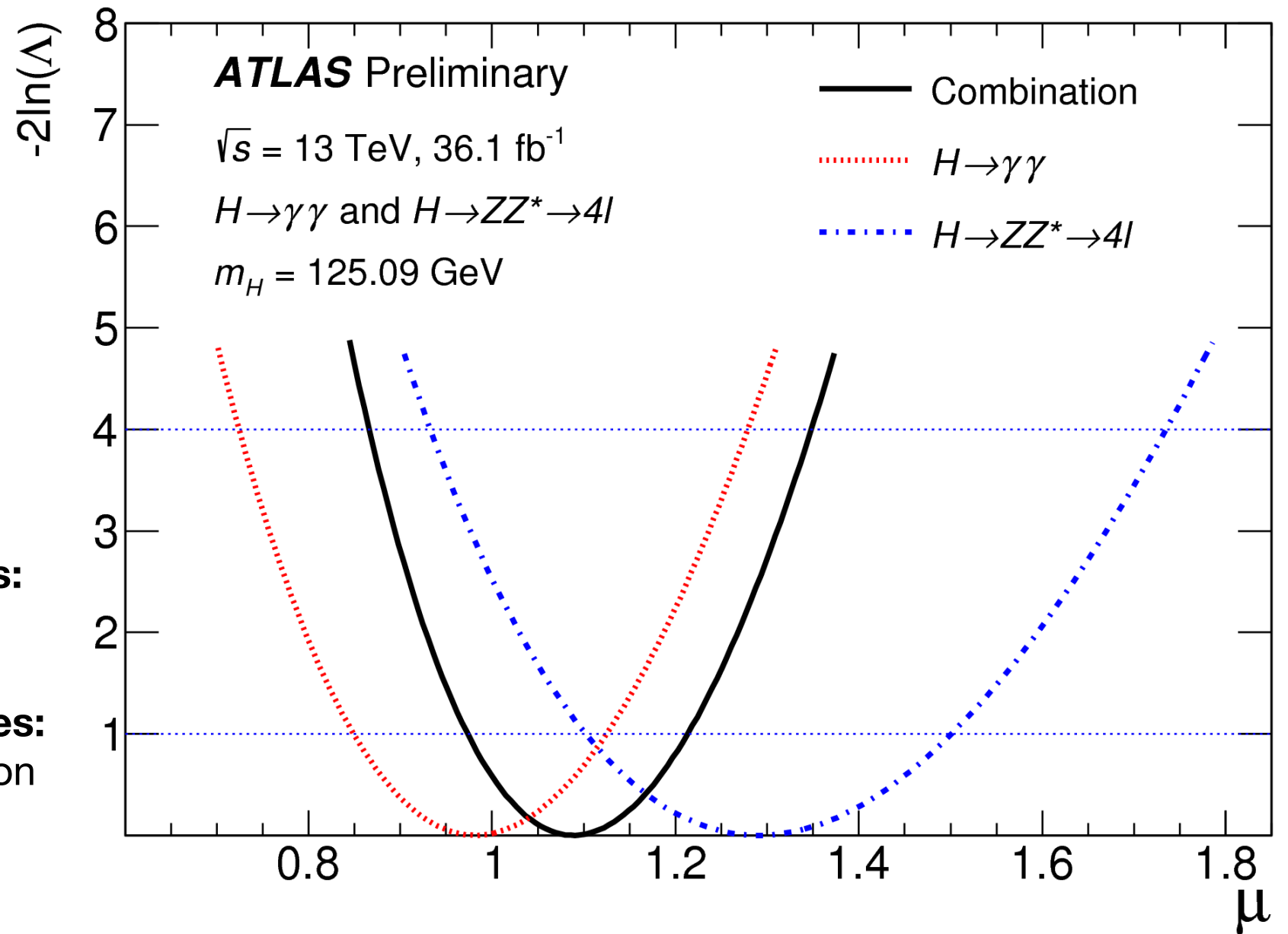
Higgs Boson global signal strength in $H \rightarrow ZZ^* \rightarrow 4\ell$ and $H \rightarrow \gamma\gamma$ channels

$$\mu = \frac{\sigma \times B}{(\sigma \times B)_{\text{SM}}}$$

Global Signal Strength:
 $\mu_H = 1.09 \pm 0.02$

Dominant theoretical uncertainties:
 QCD scale & PDF variations

Dominant experimental uncertainties:
 luminosity & electron/photon resolution



$H \rightarrow \gamma\gamma$ signal strength: $\mu = 0.99^{+0.14}_{-0.14}$

$H \rightarrow ZZ^* \rightarrow 4\ell$ signal strength: $\mu = 1.28^{+0.21}_{-0.19}$

Mass combination Systematic Uncertainties

Systematic effect	Uncertainty on $m_H^{ZZ^*}$ [MeV]
Muon momentum scale	40
Electron energy scale	20
Background modelling	10
Simulation statistics	8

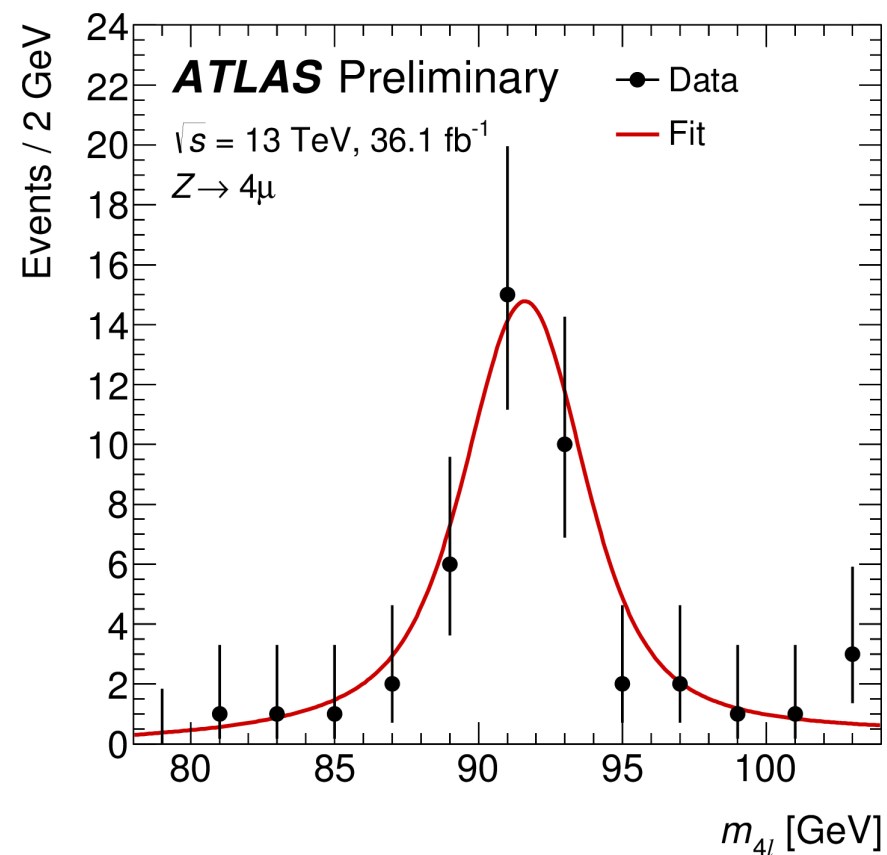
Mass combination Systematic Uncertainties

Source	Systematic uncertainty on $m_H^{\gamma\gamma}$ [MeV]
LAr cell non-linearity	± 200
LAr layer calibration	± 190
Non-ID material	± 120
Lateral shower shape	± 110
ID material	± 110
Conversion reconstruction	± 50
$Z \rightarrow ee$ calibration	± 50
Background model	± 50
Primary vertex effect on mass scale	± 40
Resolution	+20 -30
Signal model	± 20

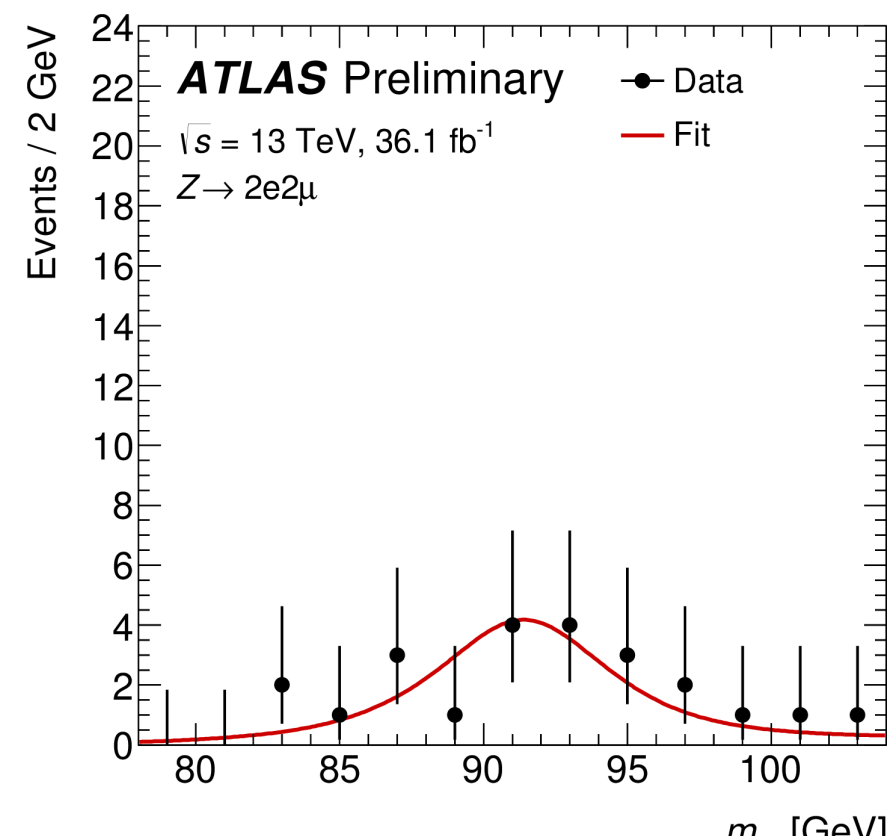
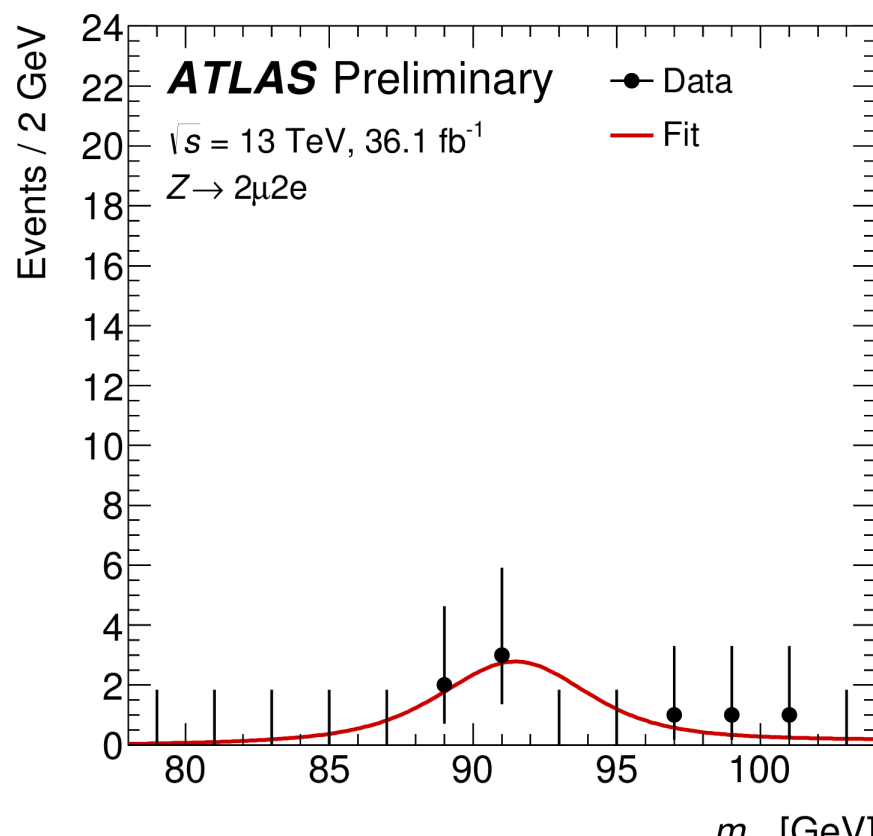
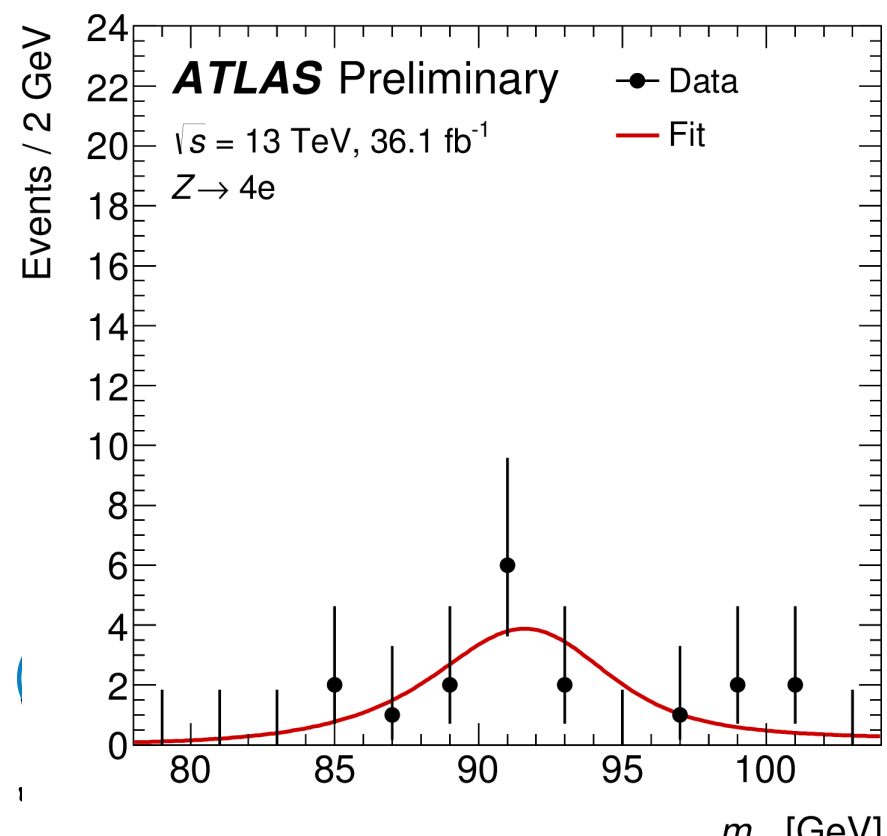
Mass combination Systematic Uncertainties

Source	Systematic uncertainty on m_H [MeV]
LAr cell non-linearity	90
LAr layer calibration	90
Non-ID material	60
ID material	50
Lateral shower shape	50
$Z \rightarrow ee$ calibration	30
Muon momentum scale	20
Conversion reconstruction	20

$H \rightarrow ZZ \rightarrow 4l$ validation of mass determination



Category	m_Z in simulation [GeV]	m_Z in data [GeV]
4μ	$91.19^{+0.41}_{-0.41}$	$91.46^{+0.42}_{-0.41}$
$4e$	$91.19^{+1.02}_{-1.03}$	$91.75^{+1.08}_{-1.06}$
$2\mu 2e$	$91.18^{+1.11}_{-1.11}$	$91.31^{+1.62}_{-1.33}$
$2e 2\mu$	$91.19^{+0.90}_{-0.90}$	$92.49^{+0.91}_{-0.94}$
Combined	$91.19^{+0.34}_{-0.34}$	$91.62^{+0.35}_{-0.35}$



H → ZZ → 4l fiducial phase space selection

Leptons and jets	
Muons:	$p_T > 5 \text{ GeV}, \eta < 2.7$
Electrons:	$p_T > 7 \text{ GeV}, \eta < 2.47$
Jets:	$p_T > 30 \text{ GeV}, y < 4.4$
Jet-lepton overlap removal:	$\Delta R(\text{jet}, \ell) > 0.1 \text{ (0.2) for muons (electrons)}$
Lepton selection and pairing	
Lepton kinematics:	$p_T > 20, 15, 10 \text{ GeV}$
Leading pair (m_{12}):	SFOS lepton pair with smallest $ m_Z - m_{\ell\ell} $
Subleading pair (m_{34}):	remaining SFOS lepton pair with smallest $ m_Z - m_{\ell\ell} $
Event selection (at most one quadruplet per channel)	
Mass requirements:	$50 \text{ GeV} < m_{12} < 106 \text{ GeV}$ and $12 \text{ GeV} < m_{34} < 115 \text{ GeV}$
Lepton separation:	$\Delta R(\ell_i, \ell_j) > 0.1 \text{ (0.2) for same- (different-)flavour leptons}$
J/ψ veto:	$m(\ell_i, \ell_j) > 5 \text{ GeV}$ for all SFOS lepton pairs
Mass window:	$115 \text{ GeV} < m_{4\ell} < 130 \text{ GeV}$

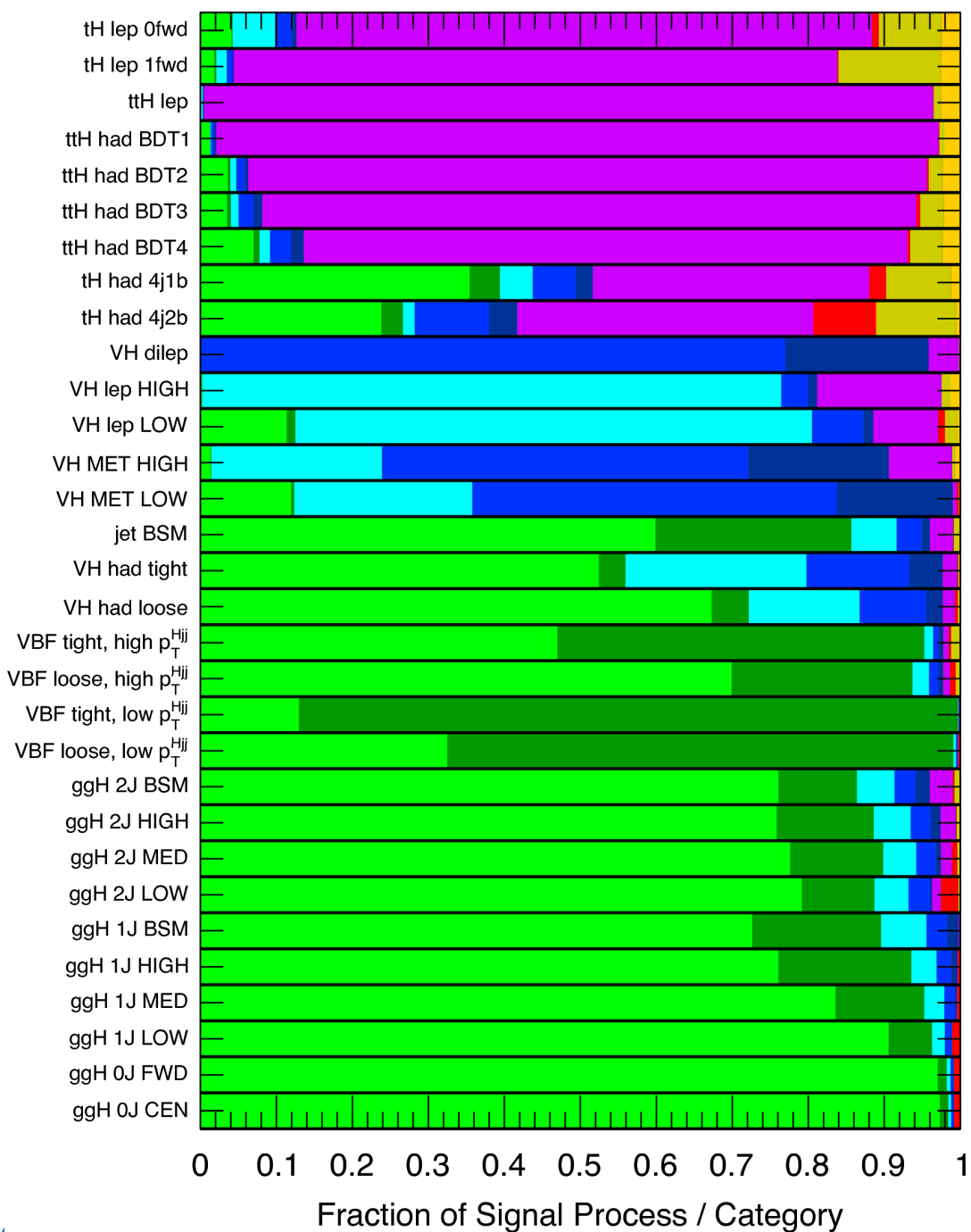
H → ZZ → 4l fiducial and total cross section uncertainties

Observable	Stat unc. [%]	Systematic unc. [%]	Dominant systematic components [%]						
			e	μ	jets	ZZ* theo	Model	Z + jets + $t\bar{t}$	Lumi
σ_{comb}	14	7	3	3	< 0.5	2	0.8	0.8	4
$d\sigma / dp_{T,4\ell}$	30–150	3–11	1–4	1–3	< 0.5	< 7	< 6	1–6	3–5
$d\sigma / dp_{T,4\ell}$ (0j)	31–52	10–18	2–5	1–4	3–16	3–8	1	2–3	3–5
$d\sigma / dp_{T,4\ell}$ (1j)	35–15	6–30	1–4	1–3	2–29	1–4	1–11	1–2	3–5
$d\sigma / dp_{T,4\ell}$ (2j)	30–41	5–21	1–3	1–3	2–19	1–5	1–7	1–2	3–5
$d\sigma / d y_{4\ell} $	29–120	5–8	2–4	2–3	< 0.5	1–2	< 1	1	3–5
$d\sigma / d \cos\theta^* $	31–100	5–8	2–4	2–3	< 0.5	1–2	< 2	1–4	3–5
$d\sigma / dm_{34}$	26–53	4–13	2–5	1–5	< 0.5	1–6	< 1	1–3	3–5
$d^2\sigma / dm_{12} dm_{34}$	21–40	4–12	2–4	1–4	< 0.5	1–6	< 1	1–4	3–5
$d\sigma / dN_{\text{jets}}$	22–44	6–31	1–4	1–3	4–22	2–4	1–22	1–2	3–5
$d\sigma / dp_{T}^{\text{lead.jet}}$	30–53	5–18	1–4	1–3	3–16	2–3	1–8	1–2	3–5
$d\sigma / d\Delta\phi_{jj}$	29–43	9–17	1–3	1–3	8–14	3–4	1–7	1	3–5
$d\sigma / dm_{jj}$	23–100	9–27	1–4	1–4	8–24	3–8	1–7	< 3	3–5

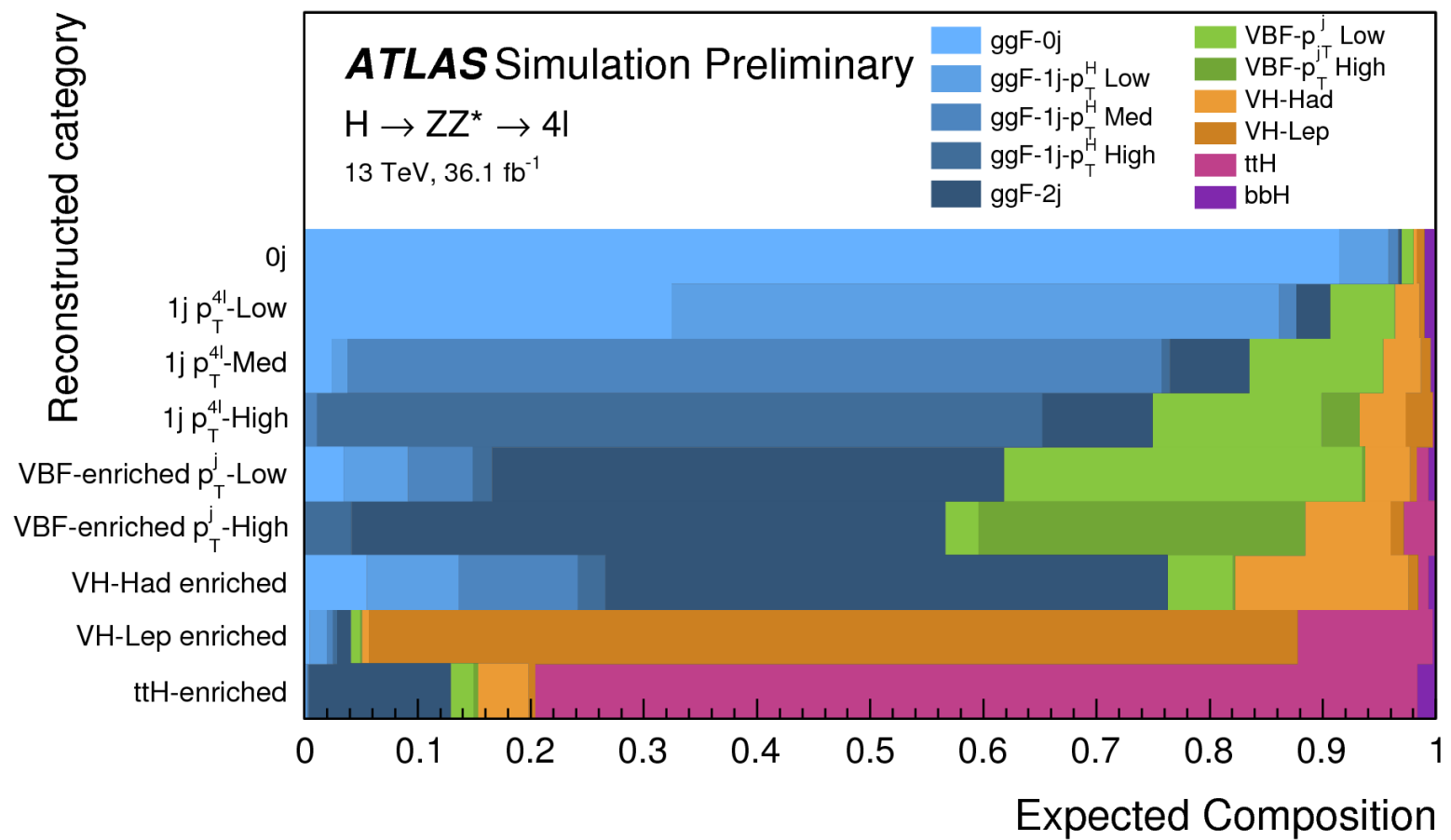
H → γγ & H → ZZ → 4l categories

■ ggH
 ■ VBF
 ■ WH
 ■ ZH
 ■ ggZH
 ■ ttH
 ■ bbH
 ■ tHqb
 ■ tHW

ATLAS Preliminary $H \rightarrow \gamma\gamma, m_H = 125.09 \text{ GeV}$



Reconstructed category

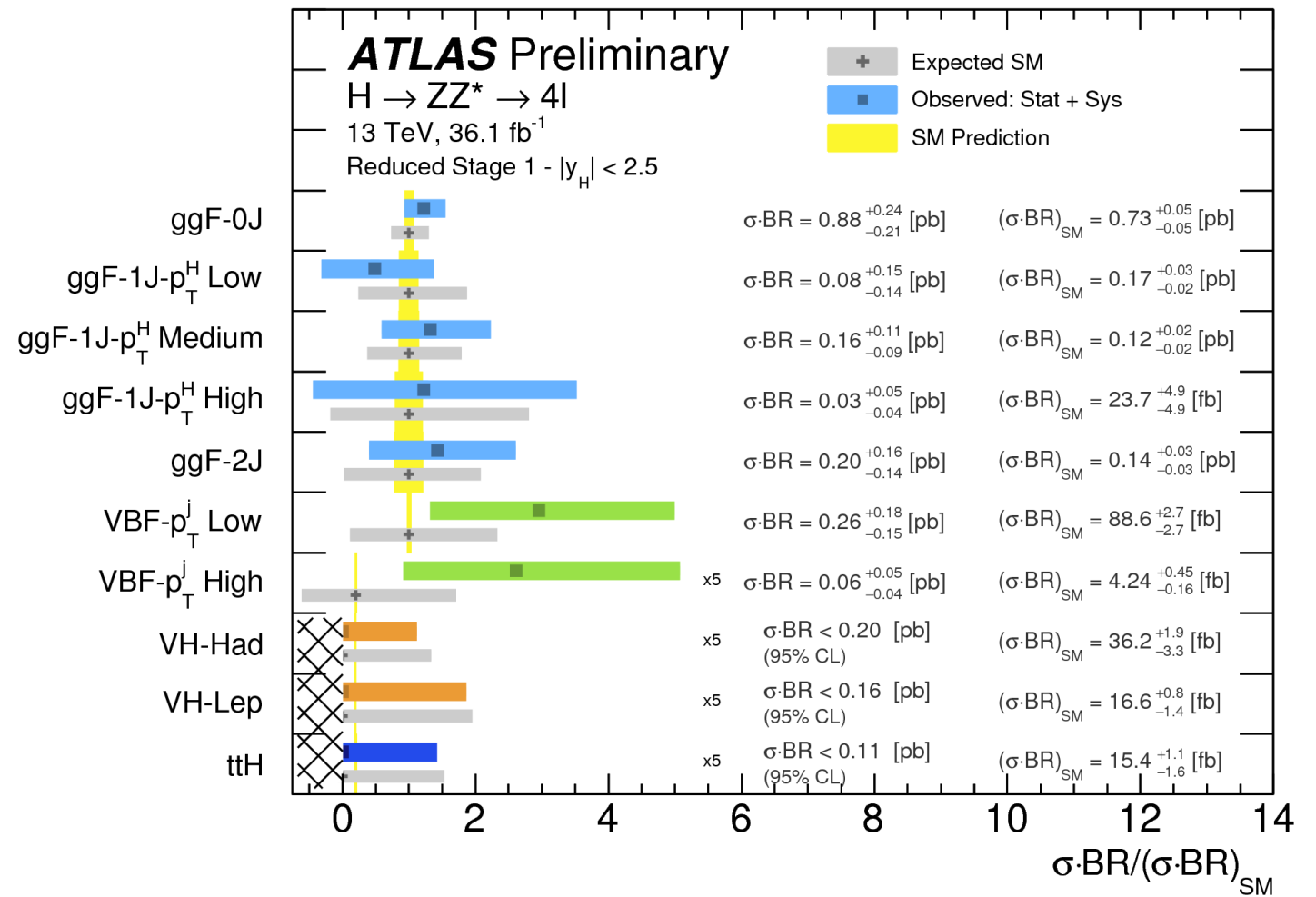
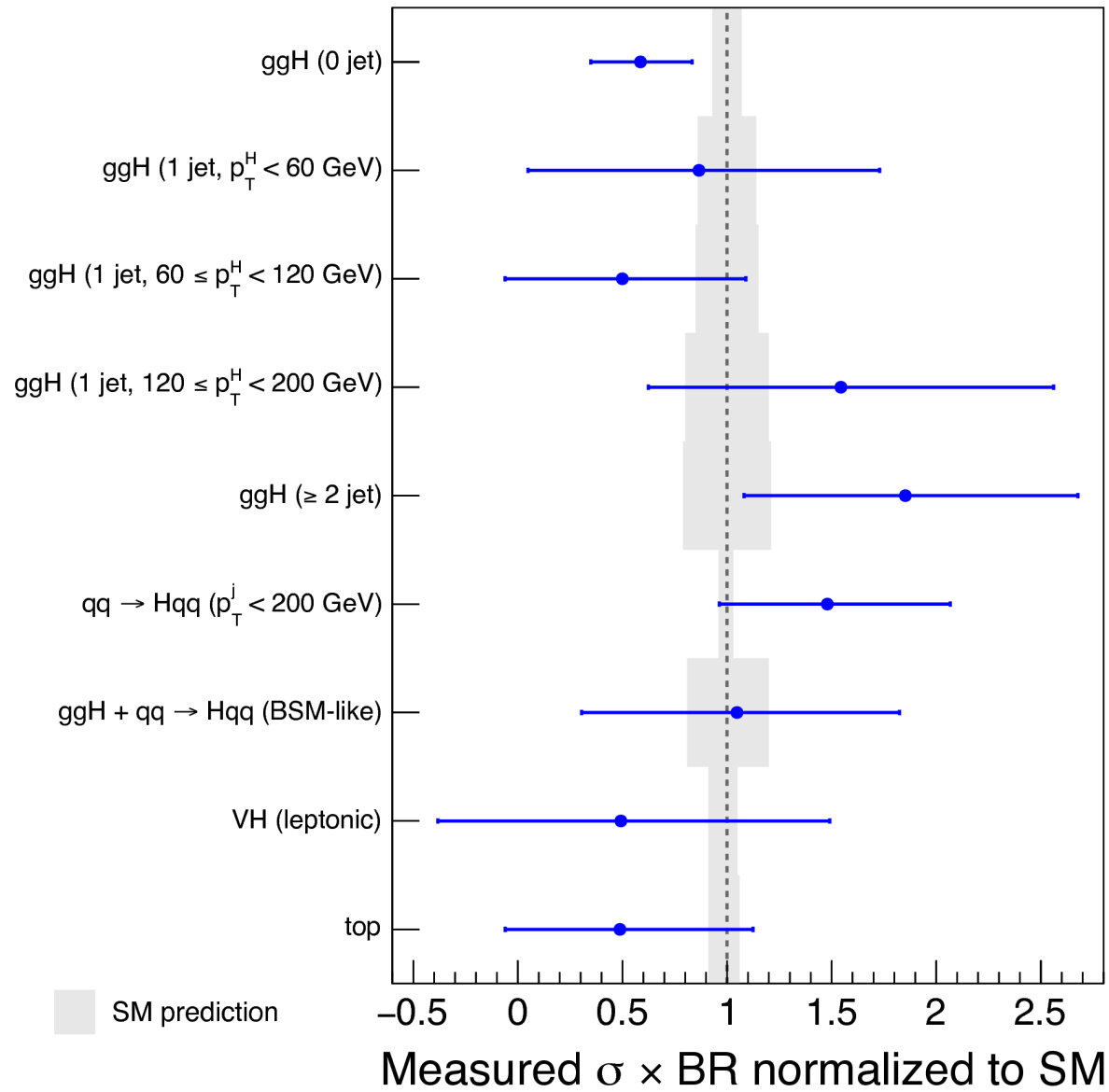


$H \rightarrow \gamma\gamma$ & $H \rightarrow ZZ \rightarrow 4\ell$ categories

$H \rightarrow \gamma\gamma$	$H \rightarrow ZZ^* \rightarrow 4\ell$
$t\bar{t}H+tH$ leptonic (two tHX and one $t\bar{t}H$ categories)	$t\bar{t}H$
$t\bar{t}H+tH$ hadronic (two tHX and four BDT $t\bar{t}H$ categories)	VH leptonic
VH dilepton	2-jet VH
VH one-lepton, $p_T^{\ell+MET} \geq 150$ GeV	2-jet VBF, $p_T^{j1} \geq 200$ GeV
VH one-lepton, $p_T^{\ell+MET} < 150$ GeV	2-jet VBF, $p_T^{j1} < 200$ GeV
VH $E_T^{\text{miss}}, E_T^{\text{miss}} \geq 150$ GeV	1-jet ggF, $p_T^{4\ell} \geq 120$ GeV
VH $E_T^{\text{miss}}, E_T^{\text{miss}} < 150$ GeV	1-jet ggF, 60 GeV $< p_T^{4\ell} < 120$ GeV
$VH+VBF$ $p_T^{j1} \geq 200$ GeV	1-jet ggF, $p_T^{4\ell} < 60$ GeV
VH hadronic (BDT tight and loose categories)	0-jet ggF
VBF, $p_T^{\gamma\gamma jj} \geq 25$ GeV (BDT tight and loose categories)	
VBF, $p_T^{\gamma\gamma jj} < 25$ GeV (BDT tight and loose categories)	
ggF 2-jet, $p_T^{\gamma\gamma} \geq 200$ GeV	
ggF 2-jet, 120 GeV $\leq p_T^{\gamma\gamma} < 200$ GeV	
ggF 2-jet, 60 GeV $\leq p_T^{\gamma\gamma} < 120$ GeV	
ggF 2-jet, $p_T^{\gamma\gamma} < 60$ GeV	
ggF 1-jet, $p_T^{\gamma\gamma} \geq 200$ GeV	
ggF 1-jet, 120 GeV $\leq p_T^{\gamma\gamma} < 200$ GeV	
ggF 1-jet, 60 GeV $\leq p_T^{\gamma\gamma} < 120$ GeV	
ggF 1-jet, $p_T^{\gamma\gamma} < 60$ GeV	
ggF 0-jet (central and forward categories)	

Higgs boson STXS cross sections measurements for $H \rightarrow ZZ^* \rightarrow 4l$ and $H \rightarrow \gamma\gamma$

ATLAS Preliminary $\sqrt{s}=13$ TeV, 36.1 fb $^{-1}$
 $H \rightarrow \gamma\gamma$, $m_H=125.09$ GeV



H → $\gamma\gamma$ fiducial definitions

Objects	Definition
Photons	$ \eta < 1.37$ OR $1.52 < \eta < 2.37$, $p_{\text{T}}^{\text{iso},0.2}/p_{\text{T}}^{\gamma} < 0.05$
Jets	anti- k_t , $R = 0.4$, $p_{\text{T}} > 30$ GeV, $ y < 4.4$
Leptons, ℓ	e or μ , $p_{\text{T}} > 15$ GeV, $ \eta < 2.47$ (excluding $1.37 < \eta < 1.52$ for $\ell = e$)
Fiducial region	Definition
Diphoton fiducial	$N_{\gamma} \geq 2$, $p_{\text{T}}^{\gamma_1} > 0.35 m_{\gamma\gamma}$, $p_{\text{T}}^{\gamma_2} > 0.25 m_{\gamma\gamma}$
VBF-enhanced	Diphoton fiducial, $N_j \geq 2$, $m_{jj} > 400$ GeV, $ \Delta y_{jj} > 2.8$, $ \Delta\phi_{\gamma\gamma,jj} > 2.6$
$N_{\text{lepton}} \geq 1$	Diphoton fiducial, $N_{\ell} \geq 1$
High $E_{\text{T}}^{\text{miss}}$	Diphoton fiducial, $E_{\text{T}}^{\text{miss}} > 80$ GeV, $p_{\text{T}}^{\gamma\gamma} > 80$ GeV
$t\bar{t}H$ -enhanced	Diphoton fiducial, $(N_j \geq 4, N_{\text{b-jets}} \geq 1)$ OR $(N_j \geq 3, N_{\text{b-jets}} \geq 1, N_{\ell} \geq 1)$

$H \rightarrow \gamma\gamma$ fiducial cross section uncertainties

Source	Uncertainty on fiducial cross section (%)				
	Diphoton	VBF-enhanced	$N_{\text{lepton}} \geq 1$	$t\bar{t}H$ -enhanced	High E_T^{miss}
Fit (stat.)	17%	22%	72%	150%	53%
Fit (syst.)	6%	8%	28%	170%	13%
Photon efficiency	1.8%	1.8%	1.8%	1.8%	1.9%
Jet energy scale/resolution	-	8.9%	-	4.5%	6.9%
b -jet flavour tagging	-	-	-	3%	-
Lepton selection	-	-	0.8%	0.2%	-
Pileup	1.1%	2.9%	1.3%	4.4%	2.5%
Theoretical modeling	4.2%	8.2%	8.7%	12.7%	30%
Luminosity	3.2%	3.2%	3.2%	3.2%	3.2%

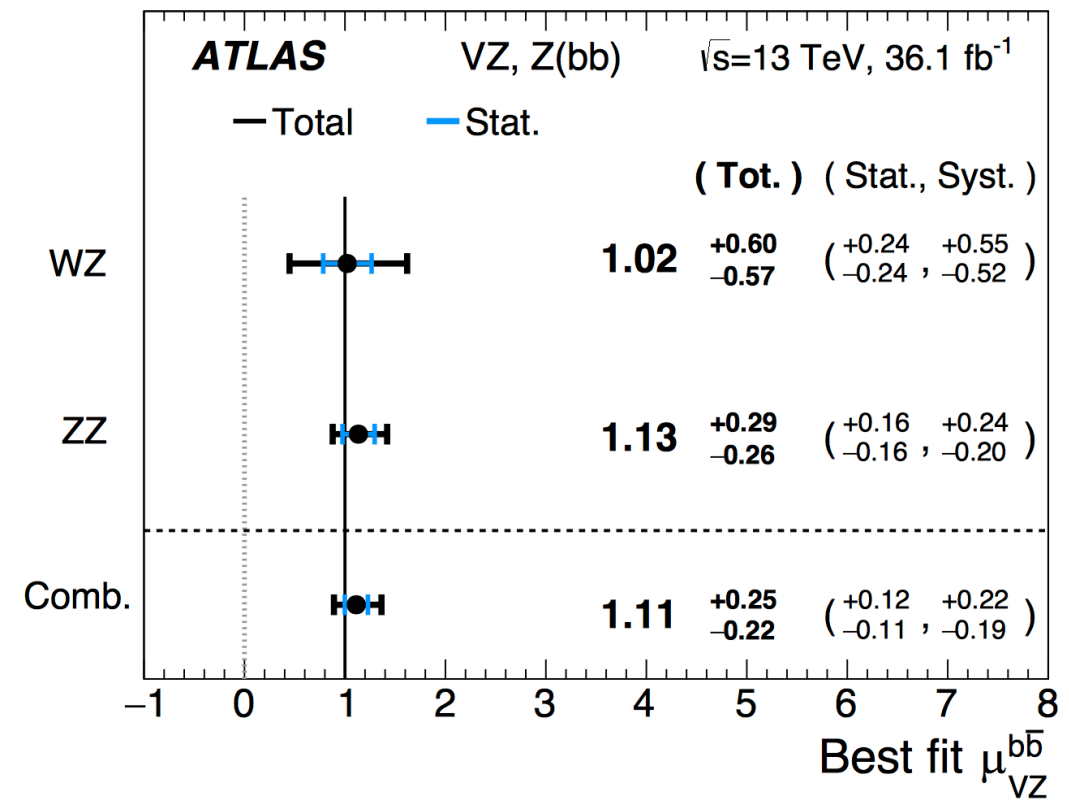
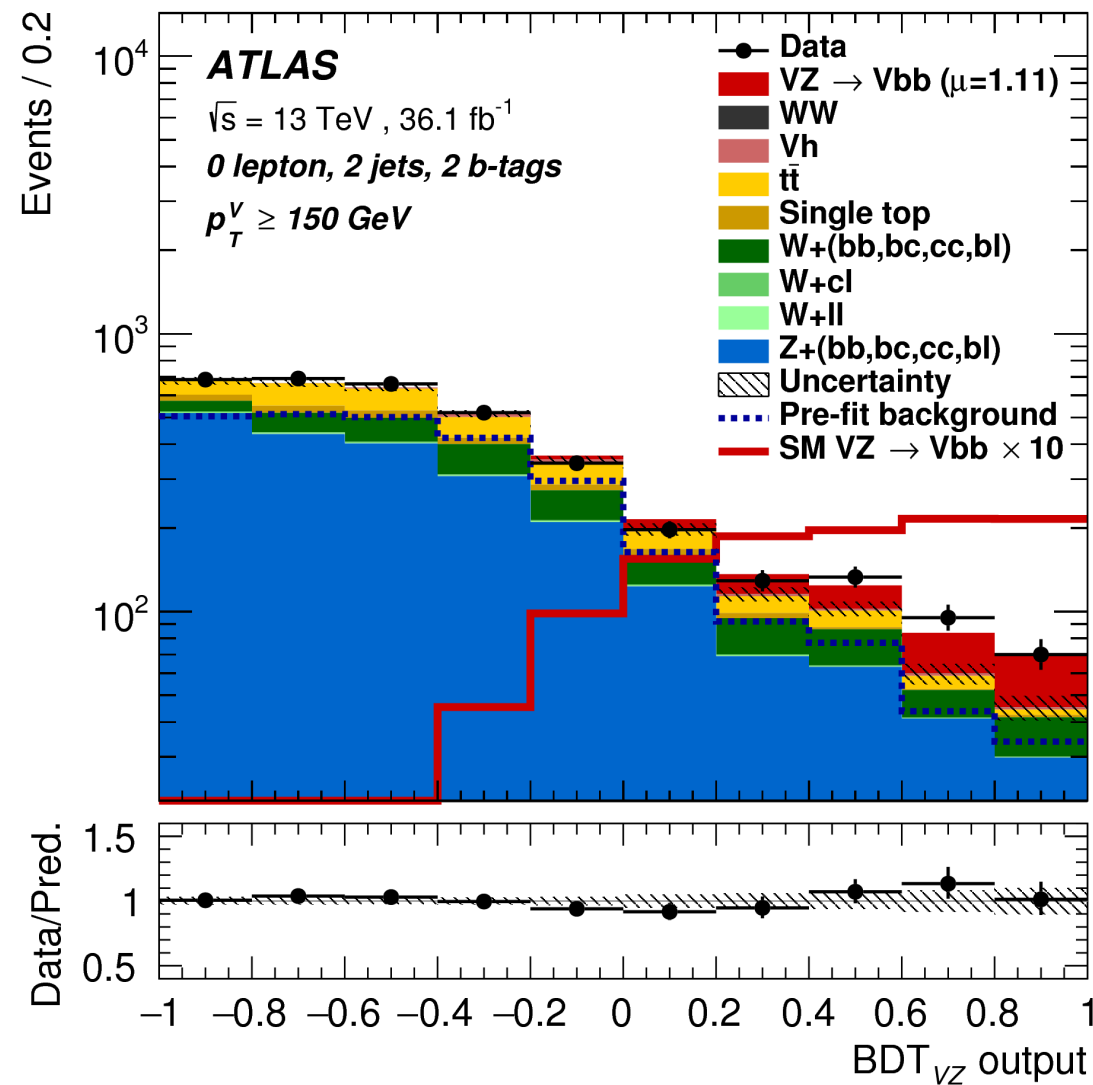
H → bb event selection

Selection	0-lepton	1-lepton		2-lepton
		e sub-channel	μ sub-channel	
Trigger	E_T^{miss}	Single lepton	E_T^{miss}	Single lepton
Leptons	0 loose leptons with $p_T > 7$ GeV	1 tight electron $p_T > 27$ GeV	1 medium muon $p_T > 25$ GeV	2 loose leptons with $p_T > 7$ GeV ≥ 1 lepton with $p_T > 27$ GeV
E_T^{miss}	> 150 GeV	> 30 GeV	–	–
$m_{\ell\ell}$	–	–	–	$81 \text{ GeV} < m_{\ell\ell} < 101 \text{ GeV}$
Jets	Exactly 2 or 3 jets			Exactly 2 or ≥ 3 jets
Jet p_T	> 20 GeV			
b-jets	Exactly 2 b-tagged jets			
Leading b-tagged jet p_T	> 45 GeV			
H_T	> 120 (2 jets), >150 GeV (3 jets)	–	–	–
$\min[\Delta\phi(\vec{E}_T^{\text{miss}}, \vec{\text{jets}})]$	> 20° (2 jets), > 30° (3 jets)	–	–	–
$\Delta\phi(\vec{E}_T^{\text{miss}}, \vec{bb})$	> 120°	–	–	–
$\Delta\phi(\vec{b}_1, \vec{b}_2)$	< 140°	–	–	–
$\Delta\phi(\vec{E}_T^{\text{miss}}, \vec{E}_{T,\text{trk}}^{\text{miss}})$	< 90°	–	–	–
p_T^V regions	> 150 GeV			(75, 150] GeV, > 150 GeV
Signal regions	✓	$m_{bb} \geq 75 \text{ GeV}$ or $m_{\text{top}} \leq 225 \text{ GeV}$		Same-flavour leptons Opposite-sign charge (μμ sub-channel)
Control regions	–	$m_{bb} < 75 \text{ GeV}$ and $m_{\text{top}} > 225 \text{ GeV}$		Different-flavour leptons

H → bb event uncertainties

Source of uncertainty		σ_μ
Total		0.39
Statistical		0.24
Systematic		0.31
<hr/>		
Experimental uncertainties		
Jets		0.03
E_T^{miss}		0.03
Leptons		0.01
<i>b</i> -tagging	<i>b</i> -jets	0.09
	<i>c</i> -jets	0.04
	light jets	0.04
	extrapolation	0.01
Pile-up		0.01
Luminosity		0.04
<hr/>		
Theoretical and modelling uncertainties		
Signal		0.17
Floating normalisations		0.07
<i>Z</i> + jets		0.07
<i>W</i> + jets		0.07
<i>t</i> \bar{t}		0.07
Single top quark		0.08
Diboson		0.02
Multijet		0.02
MC statistical		0.13

Diboson production



Clear excess of VZ, Z \rightarrow bb
5.8 σ (expected: 5.3 σ)

Dimuon expected events

	S	B	S/\sqrt{B}	FWHM	Data
Central low $p_T^{\mu\mu}$	11	8000	0.12	5.6 GeV	7885
Non-central low $p_T^{\mu\mu}$	32	38000	0.16	7.0 GeV	38777
Central medium $p_T^{\mu\mu}$	23	6400	0.29	5.7 GeV	6585
Non-central medium $p_T^{\mu\mu}$	66	31000	0.37	7.1 GeV	31291
Central high $p_T^{\mu\mu}$	16	3300	0.28	6.3 GeV	3160
Non-central high $p_T^{\mu\mu}$	40	13000	0.35	7.7 GeV	12829
VBF loose	3.4	260	0.21	7.6 GeV	274
VBF tight	3.4	78	0.38	7.5 GeV	79

Bin-by-bin unfolding

$$\sigma_{i, fid} = \sigma_i \times A_i \times BR = \frac{N_{i, fit}}{L \times C_i}$$

A_i = acceptance

C_i = correction for detector efficiency and resolution

$N_{i, fit}$ = number of signal events observed

σ_i = total cross section